AST5-CT-2006-030768

COFCLUO

Clearance of Flight Control Laws using Optimisation

Specific Targeted Research Project

1.4 Aeronautics and Space

D2.3.5 : Final report WP2.3

Due date of deliverable: January 31, 2010
Actual submission date: January 26, 2010

Start date of project: February 1, 2007 Duration: January 31, 2010

University of Siena (UNISI)

Revision V0.2

Project co-funded by the European Commission within the Sixth Framework Programme (2002-2006)		
Dissemination Level		
PU	Public	X
PP	Restricted to other programme participants (including the Commission Services)	
RE	Restricted to a group specified by the consortium (including the Commission Services)	
CO	Confidential, only for members of the consortium (including the Commission Services)	

D2.3.5 Final Report WP2.3

Andrea Garulli, Alfio Masi, Simone Paoletti, Ercüment Türkoğlu

DII, Università di Siena, Via Roma 56, 53100 Siena, Italy
Email: garulli@dii.unisi.it

Clément Roos

ONERA-DCSD, 2 avenue Edouard Belin, 31400 Toulouse, France
Email: clement.roos@onera.fr

January 26, 2010

Abstract

The report provides an extensive summary on the outcome of the research conducted within WP2.3 of the `COFCLUO` project. It addresses several clearance criteria concerning both integral (aeroelastic) and nonlinear models of a generic passenger aircraft. Clearance criteria have been formulated as robustness analysis problems. Several different techniques, based on parameter-dependent Lyapunov functions or μ-analysis, have been considered for the robustness analysis of systems with LFR uncertainty. Such techniques are applied to closed-loop LFR models, derived from the aircraft integral and nonlinear models, with the aim of finding the largest region in the uncertain parameter space and/or in the flight envelope, for which robust stability is guaranteed. The trade-off between conservatism and computational burden is analyzed on a broad selection of integral and nonlinear models for each considered technique.

Contents

I Lyapunov-based robustness analysis for clearance problems 4

1 Introduction 5

2 Robustness analysis using Lyapunov functions 6
2.1 Problem statement in LFR framework . . . 6
2.2 Wang-Balakrishnan conditions . . . 7
2.3 Fu-Dasgupta conditions . . . 8
2.4 Dettori-Scherer conditions . . . 9

3 Clearance criteria 10
3.1 Aeroelastic stability clearance criterion . . . 10
3.2 LFR models for aeroelastic stability . . . 10
3.3 Un-piloted stability of nonlinear models . . . 12
3.4 LFR models for nonlinear stability . . . 13
3.5 Progressive and adaptive tiling . . . 14
3.6 Gridding . . . 15

4 Results on aeroelastic stability of integral models 16
4.1 Progressive tiling . . . 16
4.1.1 C model . . . 16
4.1.2 OC model . . . 16
4.1.3 POC model . . . 17
4.1.4 CXcg model . . . 17
4.1.5 COXcg model . . . 17
4.1.6 MV model . . . 18
4.2 Adaptive tiling: MV model . . . 19

5 Results on un-piloted stability of nonlinear models 22
5.1 `CL_lon_nl_AC_#_b` models . . . 22
5.2 `CL_lon_nl_AC_#_a` models . . . 22
5.3 `CL_lon_nl_AC_#_c` models . . . 24
5.4 `CL_lon_nl_AC_#_d` models . . . 27
5.5 `CL_lon_nl_AC_#_e` models . . . 27

6 Final remarks 28

II μ-analysis based robustness analysis for clearance problems 31

7 Introduction 32

8 Overview of the work performed by ONERA 32

9 Incorporation in an industrial process **33**
9.1 Validation of the LFRs and evaluation of the modeling error 33
9.2 Integration of the modeling error into the bounds of the criteria 34
9.3 Description of the proposed clearance process 34
9.4 Determination of the most critical parametric combinations 36
9.5 Towards a generalized use of LFRs 36

10 Conclusion and future prospects **38**

Part I
Lyapunov-based robustness analysis for clearance problems

Authors: Andrea Garulli, Alfio Masi, Simone Paoletti, Ercüment Türkoğlu (UNISI)

1 Introduction

The aim of this report is to summarize the outcomes of WP2.3 within the COFCLUO project. The objective of WP2.3 was to develop convex optimization techniques for solving robustness analysis problems, arising in the clearance of flight control schemes.

Robustness analysis of linear systems depending on uncertain parameters has been a subject of notable interest in the systems and control community for several decades, and Lyapunov theory has played a pivotal role in this context. The development of computationally efficient techniques for solving convex optimization problems involving Linear Matrix Inequalities (LMIs) [1] has motivated research efforts towards more and more sophisticated sufficient conditions for assessing robust stability of uncertain systems.

Within the context of Lyapunov theory, robustness of linear systems can be analyzed through the search for Lyapunov functions which are either parameter independent, or parameter dependent. The notion of *quadratic stability*, namely the existence of a common quadratic Lyapunov function for all the admissible systems, allows one to address also time-varying uncertainties, but it usually leads to conservative results. This shortcoming has instigated research efforts on Lyapunov functions that are parameter-dependent. Sufficient conditions for the existence of parameter-dependent Lyapunov functions depending affinely or polynomially on the uncertain parameters have been proposed in the literature (the reader is referred to [2] and references therein). The main drawback of most of these approaches is that they either assume an affine dependence of the system on the uncertain parameters, or they consider polytopic uncertainty models given as convex combinations of known nominal models. However, in real-world systems, like flight control schemes, the dependence on the uncertain parameters is much more involved (usually rational) and is modeled by linear fractional representations (LFRs) [3].

In the literature, a number of sufficient conditions for robust stability of systems with LFR uncertainty, and based on parameter-dependent Lyapunov functions, have been proposed by several authors. Within the COFCLUO project, the attention has been focused on three specific techniques. The first one, proposed in [4], combines the constant scaling technique for LFR systems with the use of (rationally) parameter-dependent Lyapunov functions. This technique can also deal with time-varying parameters with bounded variation rate. The other two techniques considered rely on ideas from the classical multiplier approach adopted in the absolute stability theory, which finds useful applications in robustness analysis of uncertain systems [5]. While several authors propose the use of constant multipliers, less conservative conditions are usually obtained if parameter-dependent multipliers are adopted. Two different approaches along this line, which employ multi-affine parameter-dependent Lyapunov functions, have been presented in [6] and [7]. Relationships between these approaches have been investigated in [8].

The three techniques recalled above have been employed in two specific clearance problems defined within the COFCLUO project: the aeroelastic stability criterion for integral models [9] and the un-piloted stability criterion for nonlinear models [10]. Uncertain aircraft models have been provided as LFR systems derived from physical models of the aircraft [11, 12]. A large number of LFR systems have been derived, at different points of the flight envelope and with different values of the uncertain parameters, by employing the techniques described in [13–15]. The LFR models considered in this report are representative of the closed-loop longitudinal dynamics of the aircraft. The objective of the clearance problem is to find the largest region in the uncertain parameter space or in the flight envelope, for which the LFR system is robustly stable. Several relaxations of the considered Lyapunov-based robustness analysis techniques have been proposed, which rely on the choice of specific structures for the Lyapunov function and for the multipliers. Under the assumption that the uncertain parameters are time-invariant, the uncertainty domain has been partitioned in order to obtain more accurate and less conservative results. In this respect, two alternative approaches, denoted as progressive and adaptive partitioning, have been introduced.

A Graphical User Interface (GUI) based environment has been developed to facilitate a user interactive set-up for the considered clearance problems. A detailed description of the GUI and instructions for its use are provided in [16].

The document is organized as follows. In Section 2, LFR of an uncertain autonomous system is introduced and the sufficient conditions for robust stability analysis of systems in LFR form are described. Application of the above conditions to the specific clearance problems at hand is addressed in Section 3. Sections 4 and 5 present a collection of results concerning aeroelastic stability of integral models and un-piloted stability of nonlinear models, respectively. Finally, some conclusions based on the outcomes of the robustness analysis are presented in Section 6.

2 Robustness analysis using Lyapunov functions

In this section, we present several methods, for testing the robust stability of systems whose dependence on the uncertain parameters is rational, i.e. systems in LFR form. Sufficient conditions are provided in terms of a finite number of LMIs whose feasibility render the existence of a quadratic or parameter-dependent Lyapunov function. As a way to overcome the resulting computational complexity, described in terms of the number of free variables and the size of LMIs, structures of certain matrices (and multipliers) within the methods considered have been altered to yield more conservative but computationally less demanding sufficient conditions, hereafter referred to as "relaxed". These conditions offer a new approach in trading LMIs structural complexity with computational workload.

2.1 Problem statement in LFR framework

Consider the autonomous system

$$\dot{x}(t) = \mathbf{A}(\theta)x(t), \tag{1}$$

where $x \in \mathbb{R}^n$ is the state vector and $\mathbf{A}(\theta)$ is a function of the parameter $\theta \in \mathbb{R}^{n_\theta}$ according to the relation

$$\mathbf{A}(\theta) = A + B\Delta(\theta)(I - D\Delta(\theta))^{-1}C, \tag{2}$$

with

$$\Delta(\theta) = \mathbf{diag}(\theta_1 I_{s_1}, \ldots, \theta_{n_\theta} I_{s_{n_\theta}}). \tag{3}$$

and θ_i denotes the i-th component of vector θ. An equivalent linear fractional representation of the system (1)-(3) is given by:

$$\begin{cases} \dot{x}(t) = Ax(t) + Bq(t) \\ p(t) = Cx(t) + Dq(t) \\ q(t) = \Delta(\theta)p(t), \end{cases} \tag{4}$$

where $q \in \mathbb{R}^d$, $p \in \mathbb{R}^d$, with $d = \sum_{i=1}^{n_\theta} s_i$, and A, B, C, D are real matrices of appropriate dimensions. In view of the stability analysis of the LFR system (4), matrix A is assumed to be Hurwitz.

The uncertain parameter vector θ is supposed to belong to a hyper-rectangle Θ. Hereafter, we shall

refer to the 2^{n_θ} vertices of Θ as Ver[Θ]. The uncertain parameters are assumed to be constant (i.e., $\dot{\theta}(t) = 0$).
System (4) is said to be:

- *quadratically stable* if there exists a common quadratic Lyapunov function $V(x) = x^T P x$, for all matrices $\mathbf{A}(\theta)$, $\theta \in \Theta$;
- *robustly stable* if $\mathbf{A}(\theta)$ is Hurwitz, for all $\theta \in \Theta$.

Clearly, quadratic stability implies robust stability, while the converse is not true. Moreover, quadratic stability is also a sufficient condition for global exponential stability of the equilibrium $x = 0$ when the uncertain parameters θ_i are time-varying.
In the following, we briefly review several sufficient conditions for robust stability of system (4), based on parameter-dependent Lyapunov functions.

2.2 Wang-Balakrishnan conditions

In [4], several sufficient conditions for robust stability analysis of LFR systems are proposed. Here, we recall two of them, where both are formulated for the special case when uncertainties are time-invariant. A sufficient condition for quadratic stability of system (4) is stated as follows.

Proposition 2.1 (WBQ) *System* (4) *is quadratically stable if there exist* $P \in \mathbb{R}^{n\times n}$, $P = P^T > 0$ *and* $M \in \mathbb{R}^{d\times d}$, $M = M^T > 0$, *such that*

$$\begin{bmatrix} A^T P + PA + C^T MC & PB(\theta) + C^T MD(\theta) \\ B(\theta)^T P + D(\theta)^T MC & -M + D(\theta)^T MD(\theta) \end{bmatrix} < 0 \tag{5}$$

for all $\theta \in$ *Ver*[Θ], *with* $B(\theta) = B\Delta(\theta)$ *and* $D(\theta) = D\Delta(\theta)$.

To establish whether such condition is verified, one has to verify the feasibility of a set of 2^{n_θ} LMI constraints of dimension $n + d$, one LMI of dimension d and one LMI of dimension n. This results in a family of LMIs with a total number of free variables $n_{var} = \frac{d(d+1)}{2} + \frac{n(n+1)}{2}$.

A less conservative condition for robust stability of system (4), also presented in [4], exploits parameter-dependent Lyapunov functions of the form $V(x) = x^T Q(\theta)^{-1} x$ with $Q(\theta) = Q_0 + \sum_{j=1}^{n_\theta} \theta_j Q_j$.

Proposition 2.2 (WB) *System* (4) *is robustly stable if there exist* $n_\theta + 1$ *symmetric matrices* $Q_0, \ldots, Q_{n_\theta} \in \mathbb{R}^{n\times n}$, *and* $N \in \mathbb{R}^{d\times d}$, $N = N^T > 0$, *such that*

$$\begin{cases} Q(\theta) > 0 \\ \begin{bmatrix} AQ(\theta) + Q(\theta)A^T + B(\theta)NB(\theta)^T & Q(\theta)C^T + B(\theta)ND(\theta)^T \\ CQ(\theta) + D(\theta)NB(\theta)^T & D(\theta)ND(\theta)^T - N \end{bmatrix} < 0 \end{cases} \tag{6}$$

for all $\theta \in$ *Ver*[Θ].

In order to verify the condition in Proposition 2.2, it is necessary to solve a set of 2^{n_θ} LMIs of dimension n, 2^{n_θ} LMIs of dimension $n + d$, and one LMI of dimension d. The number of free variables is $n_{var} = (n_\theta + 1)\frac{n(n+1)}{2} + \frac{d(d+1)}{2}$.

It is important to note that when the uncertainty set Θ is symmetric with respect to the origin, the feasibility of the condition in Proposition 2.2 implies that the system is also quadratically stable, i.e. the LMIs (6) admit also a solution with $Q_i = 0$, $i = 1, \ldots, n_\theta$.

In order to obtain a condition which is computationally less demanding, one can reduce the number of free variables by imposing a structure on matrices M and N. For example, the choice of a diagonal M in the WBQ condition, or a diagonal N in the WB condition, can significantly speed up the solution of the LMI feasibility problem when d is much larger than n, however, at the price of a higher conservatism. Hereafter we will refer to these relaxations of the WBQ and WB conditions as *WBQ-dM condition* and *WB-dN condition*, respectively.

2.3 Fu-Dasgupta conditions

Another approach which provides sufficient conditions for robust stability, and is based on parameter-dependent Lyapunov functions, is the *parametric multiplier* approach. It can be seen as a generalization of the traditional multiplier approach, used in absolute stability theory [17], employing parameter-dependent multipliers. The main idea of the approach presented in [6], is to seek for a transfer matrix with affine structure, called affine multiplier, which, when cascaded with another matrix related to the uncertain system, will result in a strictly positive real transfer matrix. This affine multiplier can be found by solving a set of LMIs, whose feasibility guarantees the existence of a parameter-dependent multi-affine Lyapunov function for the uncertain LFR system.

In order to cast the problem into the framework adopted in [6] let us introduce the matrices

$$\begin{gathered} C(\theta) := \Delta(\theta)C = \textstyle\sum_{i=1}^{n_\theta} \theta_i C_i \\ D(\theta) := -I + \Delta(\theta)D = D_0 + \textstyle\sum_{i=1}^{n_\theta} \theta_i D_i, \end{gathered}$$

where $C_i = T_i C$, $D_0 = -I$, $D_i = T_i D$, for $i = 1, \ldots, n_\theta$, and

$$T_i = \mathbf{blockdiag}(0_{s_1}, \ldots, 0_{s_{i-1}}, I_{s_i}, 0_{s_{i+1}}, \ldots, 0_{s_{n_\theta}}).$$

A sufficient condition for robust stability of system (4) is introduced in the next result, by using a candidate Lyapunov function whose dependence on the uncertain parameter is multi-affine, i.e. $V(x) = x^T P(\theta)\, x$, where

$$P(\theta) = P_0 + \sum_{j=1}^{n_\theta} \theta_j P_j + \sum_{i=1}^{n_\theta} \sum_{j=i+1}^{n_\theta} \theta_i \theta_j P_{ij} + \ldots \tag{7}$$

is a generic multi-affine matrix function of θ.

Proposition 2.3 (FD) *System* (4) *is robustly stable if there exist* $2n_\theta + 2$ *matrices* $C_{\mu,i} \in \mathbb{R}^{d\times n}$, $D_{\mu,i} \in \mathbb{R}^{d\times d}$ *for* $i = 0, \ldots, n_\theta$ *such that*

$$\begin{bmatrix} C_i^T \\ D_i^T \end{bmatrix} \begin{bmatrix} C_{\mu,i} & D_{\mu,i} \end{bmatrix} + \begin{bmatrix} C_{\mu,i}^T \\ D_{\mu,i}^T \end{bmatrix} \begin{bmatrix} C_i & D_i \end{bmatrix} \leq 0 \tag{8}$$

for $i = 1, \ldots, n_\theta$, *and*

$$\left\{ \begin{array}{l} P(\theta) > 0 \\ \begin{bmatrix} \mathbf{A}^T(\theta)P(\theta) + P(\theta)\mathbf{A}(\theta) & \Pi_{1,2}(\theta) \\ \Pi_{1,2}^T(\theta) & \Pi_{2,2}(\theta) \end{bmatrix} < 0, \end{array} \right. \tag{9}$$

for all $\theta \in Ver[\Theta]$*, where* $P(\theta)$ *is given by* (7) *and*

$$\begin{array}{rcl} \Pi_{2,2}(\theta) & = & -\left(D_\mu(\theta)D^{-1}(\theta) + D^{-T}(\theta)D_\mu^T(\theta)\right) \\ \Pi_{1,2}(\theta) & = & P(\theta)BD^{-1}(\theta) - C_\mu^T(\theta) + C^T(\theta)D^{-T}(\theta)D_\mu^T(\theta) \end{array}$$

with

$$\begin{array}{l} C_\mu(\theta) = C_{\mu,0} + \sum_{i=1}^{n_\theta} \theta_i C_{\mu,i} \\ D_\mu(\theta) = D_{\mu,0} + \sum_{i=1}^{n_\theta} \theta_i D_{\mu,i} \ . \end{array}$$

The family of LMIs (8)-(9) is composed by $n_\theta + 2^{n_\theta}$ constraints of dimension $n + d$, and 2^{n_θ} constraints of dimension n. The total number of free variables is $n_{var} = (n_\theta + 1)(nd + d^2) + 2^{n_\theta}\left(\frac{n(n+1)}{2}\right)$, the rightmost term being due to the multi-affine parametrization of $P(\theta)$ in (7).

The number of free variables in the sufficient condition of Proposition 2.3 can be reduced by simplifying the structure of the affine parametric multiplier and/or the structure of the Lyapunov function, at the price of a higher degree of conservatism, but with significant benefits in terms of reduced computational complexity. In this paper, we will consider two possible relaxations of the FD condition:

- FD-cμ: full *constant multipliers* $C_\mu(\theta) = C_{\mu,0}$, $D_\mu(\theta) = D_{\mu,0}$ (i.e., $C_{\mu,i} = 0$, $D_{\mu,i} = 0$, for $i = 1, \ldots, n_\theta$);
- FD-cdμ: *constant diagonal multipliers*, which is the same as FD-cμ, but with nonzero elements only on the main diagonal of matrices $C_{\mu,0}$ and $D_{\mu,0}$.

Moreover, we will consider the following simplified structure for the Lyapunov function:

- common Lyapunov function (clf), $P(\theta) = P_0$;
- affine parameter dependent Lyapunov function (apdlf), $\quad P(\theta) = P_0 + \sum_{j=1}^{n_\theta} \theta_j P_j$.

2.4 Dettori-Scherer conditions

Another way to assess robust stability of system (4) by jointly using multi-affine parameter dependent Lyapunov functions and parameter-dependent multipliers has been proposed in [7]. The resulting sufficient condition can be stated as follows.

Proposition 2.4 (DS) *System* (4) *is robustly stable if there exist two matrices* S_0, $S_1 \in \mathbb{R}^{d\times d}$ *such that*

$$\left\{ \begin{array}{l} P(\theta) > 0 \\ \left[\begin{array}{cc} I & 0 \\ A & B \\ \hline 0 & I \\ C & D \end{array}\right]^T \left[\begin{array}{cc|c} 0 & P(\theta) & 0 \\ P(\theta) & 0 & 0 \\ \hline 0 & 0 & W(\theta) \end{array}\right] \left[\begin{array}{cc} I & 0 \\ A & B \\ \hline 0 & I \\ C & D \end{array}\right] < 0 \end{array} \right. \tag{10}$$

for all $\theta \in Ver[\Theta]$*, where* $P(\theta)$ *is given by* (7) *and*

$$W(\theta) = \left[\begin{array}{cc} S_1 + S_1^T & -S_0 - S_1\Delta(\theta) \\ -S_0^T - \Delta(\theta)S_1^T & S_0^T\Delta(\theta) + \Delta(\theta)S_0 \end{array} \right], \tag{11}$$

with $\Delta(\theta)$ *given by* (3).

The set of constraints (10) required to be solved for robustness certification, consists of 2^{n_θ} LMIs of dimension $(n+d)$ and 2^{n_θ} LMIs of dimension n, with a total number of free variables $n_{var} = 2d^2 + 2^{n_\theta}\left(\frac{n(n+1)}{2}\right)$. Once again, one can introduce relaxed versions of the DS condition by imposing structure on the free matrices S_0 and S_1, and/or the structure of the Lyapunov matrix. We will refer to the robustness stability test (10) with diagonal matrices S_0 and S_1 in (11), as *DS-dS condition*. Moreover, we will consider both common and affine parameter-dependent structures for the Lyapunov function, denoted by clf and apdlf, respectively.

Table 1 summarizes the sufficient conditions for robust stability presented in this section and the related LMI dimensions and number of optimization variables.

Remark 2.1 *In [8], it has been proved that the FD-cμ condition (with full constant multipliers $C_{\mu,0}$, $D_{\mu,0}$) and the DS condition (with full free matrices S_0, S_1) are equivalent. However, it is not clear at present whether one can establish a relationship between these techniques, when a more restrictive structure of the multipliers is imposed (e.g. between FD-cdμ and DS-dS). A preliminary comparison between the above methods and relaxations on some academic examples has been reported in [18].*

3 Clearance criteria

In this section, we briefly recall the considered clearance criteria and we formulate them as robustness analysis problems for the LFR models which have been derived from physical models of the aircraft.

3.1 Aeroelastic stability clearance criterion

Within the COFCLUO project, several clearance criteria have been presented in [9] for the certification process of the integral model of an aircraft [12].

The aeroelastic stability clearance criterion is described in [9, Section 4.1]. In order to clear the closed-loop model within the uncertain parameter domain, the largest real part of the closed-loop eigenvalues $(\lambda_1, \lambda_2, \cdots, \lambda_n)$ has to be negative, i.e.

$$\max_{j\in[1,n]} Re(\lambda_j) < 0,$$

for all possible values taken by the uncertain parameters. The presence of positive real eigenvalues indicates the presence of unstable modes, hence the associated regions accommodating these eigenvalues cannot be certified as cleared.

The techniques presented in Section 2 are applied to certify that the LFR models describing the aeroelastic dynamics of the aircraft satisfy the above eigenvalue criterion for all uncertain parameters and flight envelope variables, i.e. to prove that such models are *robustly* stable.

3.2 LFR models for aeroelastic stability

Several LFR models of the open-loop longitudinal dynamics of a civil aircraft have been derived in [13, 14], from a set of linear aeroelastic models dependent on:

- the mass configuration (expressed in terms of fullness of two fuel tanks and a payload);

Method	number of LMIs, [dimension]	n_{var}
WBQ	$1, \quad [d]$ $1, \quad [n]$ $2^{n_\theta}, \quad [n+d]$	$\frac{d(d+1)}{2} + \frac{n(n+1)}{2}$
WBQ-dM	$1, \quad [d]$ $1, \quad [n]$ $2^{n_\theta}, \quad [n+d]$	$d + \frac{n(n+1)}{2}$
WB	$1, \quad [d]$ $2^{n_\theta}, \quad [n]$ $2^{n_\theta}, \quad [n+d]$	$\frac{d(d+1)}{2} + (n_\theta+1)\frac{n(n+1)}{2}$
WB-dN	$1, \quad [d]$ $2^{n_\theta}, \quad [n]$ $2^{n_\theta}, \quad [n+d]$	$d + (n_\theta+1)\frac{n(n+1)}{2}$
FD (mapdlf)	$2^{n_\theta}, \quad [n]$ $n_\theta 2^{n_\theta}, \quad [n+d]$	$(n_\theta+1)(nd+d^2) + 2^{n_\theta}\left(\frac{n(n+1)}{2}\right)$
FD (apdlf)	$2^{n_\theta}, \quad [n]$ $n_\theta 2^{n_\theta}, \quad [n+d]$	$(n_\theta+1)(nd+d^2) + (n_\theta+1)\left(\frac{n(n+1)}{2}\right)$
FD (clf)	$2^{n_\theta}, \quad [n]$ $n_\theta 2^{n_\theta}, \quad [n+d]$	$(n_\theta+1)(nd+d^2) + \frac{n(n+1)}{2}$
FD-cμ (mapdlf)	$2^{n_\theta}, \quad [n]$ $n_\theta 2^{n_\theta}, \quad [n+d]$	$(nd+d^2) + 2^{n_\theta}\left(\frac{n(n+1)}{2}\right)$
FD-cμ (apdlf)	$2^{n_\theta}, \quad [n]$ $n_\theta 2^{n_\theta}, \quad [n+d]$	$(nd+d^2) + (n_\theta+1)\left(\frac{n(n+1)}{2}\right)$
FD-cμ (clf)	$2^{n_\theta}, \quad [n]$ $n_\theta 2^{n_\theta}, \quad [n+d]$	$(nd+d^2) + \frac{n(n+1)}{2}$
FD-cdμ (mapdlf)	$2^{n_\theta}, \quad [n]$ $n_\theta 2^{n_\theta}, \quad [n+d]$	$\min(n,d) + d + 2^{n_\theta}\left(\frac{n(n+1)}{2}\right)$
FD-cdμ (apdlf)	$2^{n_\theta}, \quad [n]$ $n_\theta 2^{n_\theta}, \quad [n+d]$	$\min(n,d) + d + (n_\theta+1)\left(\frac{n(n+1)}{2}\right)$
FD-cdμ (clf)	$2^{n_\theta}, \quad [n]$ $n_\theta 2^{n_\theta}, \quad [n+d]$	$\min(n,d) + d + \frac{n(n+1)}{2}$
DS (mapdlf)	$2^{n_\theta}, \quad [n]$ $2^{n_\theta}, \quad [n+d]$	$2d^2 + 2^{n_\theta}\left(\frac{n(n+1)}{2}\right)$
DS (apdlf)	$2^{n_\theta}, \quad [n]$ $2^{n_\theta}, \quad [n+d]$	$2d^2 + (n_\theta+1)\left(\frac{n(n+1)}{2}\right)$
DS (clf)	$2^{n_\theta}, \quad [n]$ $2^{n_\theta}, \quad [n+d]$	$2d^2 + \frac{n(n+1)}{2}$
DS-dS (mapdlf)	$2^{n_\theta}, \quad [n]$ $2^{n_\theta}, \quad [n+d]$	$2d + 2^{n_\theta}\left(\frac{n(n+1)}{2}\right)$
DS-dS (apdlf)	$2^{n_\theta}, \quad [n]$ $2^{n_\theta}, \quad [n+d]$	$2d + (n_\theta+1)\left(\frac{n(n+1)}{2}\right)$
DS-dS (clf)	$2^{n_\theta}, \quad [n]$ $2^{n_\theta}, \quad [n+d]$	$2d + \frac{n(n+1)}{2}$

Table 1: Sufficient conditions for robustness analysis.

- the trim flight point (characterized by Mach number and conventional air speed).

In order to generate closed-loop models, these LFRs have been combined with the LFRs describing the longitudinal axis actuators, sensors and the controller dynamics, by employing software tools for LFR object manipulation [19], [20]. Depending on the parameters θ appearing in the uncertainty block Δ, several different closed-loop LFR models have been considered. For some of these models, generated in the frequency range $[0, 15]$ rad/sec, the number of states n, the size d of the associated Δ-block, and the sizes s_i of the uncertainty sub-blocks associated with the Central tank (C), Outer tank (O), Payload (P), Mach number (M), conventional air speed (V) and the position of the center of gravity along the longitudinal axis (Xcg), are summarized in Table 2. Each one of the fuel load parameters and/or flight point values not appearing among the uncertain parameters θ in Table 2, are fixed to the following constant values: $C = 50\%$ $P = 0\%$, $O = 50\%$; $M = 0.86$, $V = 310$ kt, $Xcg = 0$.

Model	n	d	θ_1, $s1$	θ_2, $s2$	θ_3, $s3$	θ_{s4}, $s4$
C	20	16	C, 16	–	–	–
CXcg	20	18	C, 14	–	–	Xcg, 4
OC	20	50	C, 26	O, 24	–	–
OCXcg	20	50	C, 24	O, 22	–	Xcg, 4
POC	20	79	C, 42	O, 24	P, 13	–
MV	20	54	M, 26	V, 28	–	–

Table 2: Longitudinal closed-loop LFR models: uncertainty structure.

For the MV model, bounds on the flight parameters θ are available in terms of a polytope Θ, representing the considered flight envelope (the polytope bounded by the black line in Figures 1-3). For models C, OC and POC, the fuel load (C and O) and payload (P) ratios take values between 0 and 1. Hence, the uncertain parameter domain Θ for each of these models is, correspondingly, the interval $[0, 1]$, a square and a cube whose sides are intervals $[0, 1]$. In models CXcg and OCXcg, the position of center of gravity (Xcg) varies within the range 0 and 1, therefore, the uncertain parameter domain Θ comprise a square and a cube, each of them being with sides of unit length.

3.3 Un-piloted stability of nonlinear models

Within the COFCLUO project, several clearance criteria have been presented in [10] for the certification process of the closed-loop nonlinear model of an aircraft [11].

The un-piloted stability clearance criterion is described in [10, Section 4.1]. It requires that the closed-loop system remains stable, for all admissible values of the position of the center of gravity assumed by the control law, and for all possible trimmed point values. Because of the presence of pilot-in-the-loop control, the stability requirement can be relaxed to include slowly divergent modes, provided that the time of doubling of the divergent variables is more than 6 sec.. When the closed-loop system is represented by an LFR model as (1)-(2), this corresponds to verify that the largest real part of the eigenvalues of the closed-loop matrix $\mathbf{A}(\theta)$ is smaller than $\log(2)/6$. Notice that, due to the structure of $\mathbf{A}(\theta)$ in (2), this can be imposed by simply replacing the open-loop matrix A by the shifted matrix $A - \frac{\log(2)}{6} I$. Hereafter, this relaxed stability condition will be referred to as “weak stability”.

Due to the presence of saturations and rate limiters in the aircraft actuators, the Δ block of the resulting LFR models contains both uncertain parameters and memoryless nonlinearities (dead-zones). In the following, we will consider two different un-piloted stability clearance problems.

- LFR models containing only flight envelope variables and/or uncertain parameters in the Δ block, with dead-zones set to their nominal values (which corresponds to assuming that actuator saturations are not active): in this case, all the robustness analysis techniques described in Section 2 can be applied.

- LFR models containing dead-zones in the Δ block: in this case, dead-zones are treated as sector-bounded time-varying uncertainties, within the sector $[0, 1]$. Therefore, the robustness analysis techniques of Section 2 can still be applied, provided that a common Lyapunov function and parameter-independent multipliers are chosen.

Less conservative Lyapunov-based conditions for dealing with LFR models with dead-zones have been recently proposed in [21, 22]. However, they do not consider the presence of time-invariant parametric uncertainties in the LFR structure.

3.4 LFR models for nonlinear stability

The longitudinal nonlinear aircraft dynamics is described by the LFR models developed in [14] and successively modified in [15]. There are 16 different models corresponding to different regions of the flight envelope. The flight parameters are treated as linear time-invariant uncertain parameters. The actuator saturations are transformed into dead-zones in the LFR models. The full model includes four flight parameters (mach number, conventional air speed, aircraft mass, center of gravity) and eight dead-zones (four related to the elevator and four to the trimmable horizontal stabilizer). Table 3 summarizes the dimensions s_i of the Δ block corresponding to the flight parameter θ_i, in some of the complete closed-loop LFR models. All the dead-zones enter in the Δ block with dimension 1. The meaning of parameter symbols is explained in Table 4.

Model number	n	$mach$, $s1$	V_{CAS}, $s2$	cg, $s3$	m, $s4$
1	14	46	37	37	21
2	14	38	45	23	35
5	14	38	45	23	35
6	14	38	45	37	21
9	14	38	40	22	35
10	14	38	41	36	21
13	14	38	40	36	21
14	14	30	48	22	35

Table 3: Longitudinal nonlinear closed-loop LFR models: uncertainty structure.

Since the full models have Δ blocks of dimension up to 141, with 4 uncertain parameters and eight dead-zones, a collection of simpler models have been considered in order to speed up the robustness analysis. The dead-zones related to the trimmable horizontal stabilizer have been set to their nominal values (assuming the related position and rate limiters as not active). Then, five

Symbol	Description
m	mass
V_{CAS}	conventional air speed
cg	center of gravity
$mach$	Mach number
PA_DQ_DZ	dead-zone related to elevator position limiter in the aircraft
PC_DQ_DZ	dead-zone related to elevator position limiter in the controller
RA_DQ_DZ	dead-zone related to elevator rate limiter in the aircraft
RC_DQ_DZ	dead-zone related to elevator rate limiter in the controller

Table 4: Parameter symbols used in the model description.

different simplified LFR model classes have been defined, by considering only a subset of uncertain flight parameters and/or elevator dead-zones in the full LFRs, and setting the remaining ones to the corresponding nominal values. For notational convenience, the simplified models are name-coded in the following format:

`CL_lon_nl_AC_number_class`

where `number` refers to the Model Number reported in Table 3, while `class` characterizes the set of uncertain flight parameters or dead-zones θ_i in the model, according to Table 5. For exam-

`class`	θ_1	θ_2	θ_3	θ_4
a	$mach$	V_{CAS}		
b	cg	m		
c	PA_DQ_DZ	PC_DQ_DZ	RA_DQ_DZ	RC_DQ_DZ
d	cg	m	PA_DQ_DZ	PC_DQ_DZ
e	$mach$	V_{CAS}	PA_DQ_DZ	PC_DQ_DZ

Table 5: Simplified LFR model classes.

ple, for all models in the class `CL_lon_nl_AC_number_a`, the values of cg and $mach$ are set to the nominal values reported in [15], while the values of all the dead-zones are set to 0 (corresponding to assuming that the related actuator saturations and rate limiters are not active).

3.5 Progressive and adaptive tiling

Since all the conditions presented in Section 2 are only sufficient, they may be too conservative to clear the entire uncertainty domain, but they may succeed in clearing portions of this domain. This is still acceptable for the considered criteria, because the uncertain flight parameters are assumed to be time-invariant. This has motivated the formulation of two approaches, namely the *progressive tiling* and the *adaptive tiling*, which rely on partitioning of the uncertainty domain. These are described next.

In the progressive tiling, the idea is to progressively partition the flight/uncertainty domain Θ

into hyperbox regions (hereafter, *tiles*), and then, apply the robustness analysis conditions presented in Section 2 to each tile. The clearance procedure starts with a coarse tiling of the domain and is carried out by successively reducing the sizes of the uncleared tiles; this step involves bisection of each side of an uncleared tile. The size of each uncleared tile is reduced until the whole domain is cleared, or the predefined maximum number of bisection steps is reached. In all the performed numerical tests, the initial tile has been set equal to the whole uncertainty domain (or a hyper-rectangle containing the actual flight domain, for models whose flight envelope is a generic polytope). For each tile, the LFR system (4) has been re-parameterized, so that the resulting uncertainty region is centered in the origin of the normalized uncertainty space. If the LFR contains memoryless nonlinearities, such as dead-zones, these are treated as sector-bounded time-varying uncertainties. Hence, partitioning is not performed with respect to the corresponding parameters, but only with respect to the time-invariant flight parameters (if there are any in the considered model).

With the objective of improving the efficiency of the clearance process, one may choose to combine progressive tiling with an *adaptive* choice of the clearance condition. The idea is to proceed as in the progressive tiling approach, but to change the robustness condition when a predefined partitioning level has been reached. For example, one may first employ conservative (but fast) methods in the attempt to clear large regions of the uncertainty domain which are "easy" (in the sense that they can be cleared by conservative techniques). Then, in a second stage, one can employ more powerful (and more computationally demanding) techniques only for smaller "difficult" tiles, namely, those that have not been cleared by the first technique. In order to test this idea, adaptation with respect to the choice of the Lyapunov function has been considered and implemented in the clearance software (clearly, adaptation with respect to the multipliers structure can also be considered). The user can choose up to three different classes of LFs (constant, affine, multi-affine) and decide to switch from the simplest one to the more complex, as long as the partitioning of the uncertainty domain (Θ) continues. Application of this procedure to the clearance of the integral MV closed-loop LFR model is presented in Subsection 4.2.

3.6 Gridding

The flight/uncertainty domain of interest may contain models which are unstable. Since a model corresponds to an aircraft configuration with known values for the uncertain parameters and fixed values for the flight parameters, such unstable models will render the entire flight/uncertainty domain unclearable. Hence, in order to save computational time, before attempting to clear each tile by applying one of the selected method presented in Section 2, a gridding of the tile is performed. This involves a selection of r^{n_θ} models within the tile, chosen on a uniformly spaced grid (in the tests presented in the next sections, r has been set equal to 10). If any one of these models is found to be unstable, clearance of the tile is not attempted and the tile containing the model is temporarily marked as unstable. Conversely, if there are no unstable models within the tile grid then the selected clearance method is applied. Notice that as the partitioning of the domain proceeds, tiles that have been marked as unstable are successively partitioned and portions of them can be later cleared. When the maximum number of partitions is reached, the tiles containing unstable models found by gridding are finally marked as unstable. Clearly, by suitably defining the maximum number of partitions (and hence the minimum tile size), one can obtain an approximation to the desired precision of the domain which can be cleared by the considered robustness analysis technique.

4 Results on aeroelastic stability of integral models

This section presents a collection of results on aeroelastic stability of several closed-loop integral LFR models generated in the frequency range $[0, 15]$ rad/sec and representative of the longitudinal dynamics of an aircraft. The considered models are those reported in Table 2.

The computations were performed with 64-bit Matlab 2007b, running under Linux Ubuntu, on a PC-station equipped with an Intel XEON 5150 processor and 4 Gbyte of DDRII RAM.

4.1 Progressive tiling

We first present results obtained by applying the techniques in Section 2 with progressive tiling and maximum number of partitions set to 6 (corresponding to a minimum tile side equal to $\frac{1}{64}$ of the corresponding initial side of the uncertainty domain).

4.1.1 C model

Table 6 summarises clearance results for model C obtained by applying the progressive tiling approach with different robustness analysis conditions, and different structure of the Lyapunov function (clf and apdlf). The first column (Rate) represents the portion of the uncertainty segment $[0, 1]$ which has been cleared; the second column (NOPs) denotes the number of convex optimization problems that have been solved (corresponding to the number of tiles attempted to be cleared), while the third column provides the corresponding computational times (in seconds).

Method	Rate	NOPs	Time (sec)
DS (clf)	1	1	9.7820
DS (apdlf)	1	1	10.9726
DS-dS (clf)	1	3	10.155
DS-dS (apdlf)	1	1	4.1577
FD-cμ (clf)	1	1	5.8172
FD-cμ (apdlf)	1	1	8.7717
FD-cdμ (clf)	1	3	8.4335
FD-cdμ (apdlf)	1	1	4.9377
WBQ-dM	1	3	4.3888

Table 6: Progressive tiling: C model.

4.1.2 OC model

Results from the robustness stability analysis carried out on the model OC are shown in Table 7 (note that here times are expressed in hours).

It can be seen that the methods and relaxations that had been employed have managed to certify robust stability of both C and OC model within the whole uncertainty domain. As expected, the conditions involving affine parameter-dependent Lyapunov functions (apdlf) have to solve in general a smaller number of optimization problems, with respect to those formulated with common Lyapunov functions (clf). Nevertheless, this leads to a reduction of the computational time only if

Method	Rate	NOPs	Time (hours)
DS-dS (clf)	1	73	0.4424
DS-dS (apdlf)	1	41	0.5311
FD-cμ (clf)	1	33	2.9252
FD-cμ (apdlf)	1	1	0.1032
FD-cdμ (clf)	1	85	0.3668
FD-cdμ (apdlf)	1	49	0.5308
WBQ-dM	1	169	0.2468

Table 7: Progressive tiling: OC model.

the number of solved optimization problems turns out to be significantly smaller (in this respect, see e.g. the different behavior of FD-cμ and FD-cdμ for model OC). Comparison of different relaxations of the same method indicates that reducing the number of free variables by choosing structurally simpler multipliers, can increase the time required for robustness certification if the number of optimization problems to be solved grows too much (for example, this is the case of FD relaxations with apdlf for model OC).

4.1.3 POC model

Table 8 presents performance indicators of the stability analysis performed on the POC model by adopting the progressive tiling approach. It can be observed that, as the number of uncertain parameters θ and the size of the uncertainty block $\Delta(\theta)$ grow, the computational workload increases significantly. The considered techniques have managed to clear the entire uncertainty domain. Other techniques have been tested, e.g. using apdlf instead of clf, but they turned out to be significantly more computationally demanding.

Method	Rate	NOPs	Time (hours)
DS-dS (clf)	1	993	33.7136
FD-cμ (clf)	1	105	142.6362

Table 8: Progressive tiling: POC model.

4.1.4 CXcg model

Table 9 compiles clearance analysis data for the LFR model with C and Xcg uncertain values in the Δ-block. All the considered techniques have managed to clear the entire 2-D uncertainty domain. Note that an increase in the number of OPs solved also increases computational overhead (where computational times are expressed in seconds).

4.1.5 COXcg model

Table 10 presents results from the progressive clearance analysis performed on COXcg closed-loop LFR model.

Method	Rate	NOPs	Time (seconds)
DS (clf)	1	1	30.8872
DS (apdlf)	1	1	44.4729
DS-dS (clf)	1	5	48.5942
DS-dS (apdlf)	1	1	16.3342
FD-cμ (clf)	1	1	18.6065
FD-cμ (apdlf)	1	1	32.3051
FD-cdμ (clf)	1	5	32.3783
FD-cdμ (apdlf)	1	1	18.918
WBQ-dM	1	5	9.1653

Table 9: Progressive tiling: CXcg model.

Method	Rate	NOPs	Time (hours)
DS (clf)	1	185	327.008
DS (apdlf)	1	1	3.1230
DS-dS (clf)	1	745	11.1694
DS-dS (apdlf)	1	265	10.8935
FD-cμ (clf)	1	185	41.5262
FD-cμ (apdlf)	1	1	0.2965
FD-cdμ (clf)	1	841	8.8738
FD-cdμ (apdlf)	1	385	13.5763
WBQ-dM	1	2129	4.57005

Table 10: Progressive tiling: COXcg model.

Notable is that theoretically more conservative relaxations, although in need of significantly higher number of LMI optimization problem runs, have proved to be less computationally demanding with respect to their less conservative forms. Hence, an increase in the number of free variables (e.g. DS and FD-cμ) has indeed reduced the number of optimization problems solved, however, have resulted in computationally more involved optimization problems.

It is also interesting to note that in Tables 6, 9 and 10, the times elapsed for clearance by DS method are always larger than those employed by FD-cμ (recall that the two methods are equivalent, see Remark 2.1). This seems to suggest that the parametrization of the FD-cμ condition is more efficient.

4.1.6 MV model

Table 11 presents results on robust stability analysis for the MV model.

Progressive tiling has been employed in the assessment of the flight envelope. The maximum number of partitions has been increased to 7, since this is the first example in which the clearance rate is not equal to 1 for all the considered techniques. It is worth remarking that the Rate is computed as the ratio of the cleared domain and the portion of the domain which does not

Method	Rate	NOPs	Time (h:m:s)	Time/OP (h:m:s)
DS-dS (clf)	0.9875	1282	12 : 32 : 13	0 : 0 : 35
DS-dS (apdlf)	0.9931	1030	24 : 35 : 25	0 : 1 : 25
FD-cμ (clf)	0.9993	218	34 : 0 : 29	0 : 9 : 21
FD-cμ (apdlf)	1	174	30 : 9 : 45	0 : 10 : 24
FD-cdμ (clf)	0.9895	1346	8 : 28 : 2	0 : 0 : 22
FD-cdμ (apdlf)	0.9921	1202	20 : 59 : 54	0 : 1 : 2

Table 11: Progressive tiling: `MV` model.

contain unstable models found by gridding. This means that it can be interpreted as a measure of effectiveness of the considered technique (when the rate is less than 1, there are regions that could not be cleared even if the gridding was not able to find unstable models).

By inspecting the results in Table 11 one can observe that, while an increase in the number of free variables (e.g. from FD-cdμ to FD-cμ) has led to a reduction in the number of optimization problems solved, this has not translated into computationally less demanding optimization problems. However, it is notable that the least conservative and most computationally demanding method (FD-cμ with apdlf) was the only one able to clear the entire flight envelope.

Figures 1-3 offer a detailed picture of the certified regions provided by the considered techniques. The red tiles contain closed-loop models that have been found to be unstable by gridding; the green tiles show the areas which have been cleared, and the white tiles indicate the regions which have neither been cleared nor found to contain unstable models by gridding. The different tiling patterns testify the different level of conservatism of the relaxations. It can be seen that the condition FD-cμ in Figure 2 provides the largest cleared region, and was the only one to completely clear the actual flight envelope (denoted by the polytope in black). Clearly, a more precise approximation of the robust stability domain boundary can be obtained by further reducing the minimum tile size.

4.2 Adaptive tiling: MV model

The adaptive procedure described in Subsection 3.5 has been tested on the model MV, and the adaptation has been performed on the structure of the Lyapunov function. The conditions DS-dS, FD-cμ and FD-cdμ have been first applied with progressive tiling with a common Lyapunov function; then, the same relaxations with an affine parameter-dependent Lyapunov function have been applied to the tiles previously uncleared. Table 12 reports the clearance results obtained for the model MV by employing the adaptive tiling. Columns 2 and 3 in Table 12 indicate the number of bisections for which the clf and apdlf conditions have been employed, respectively. For example, clf=2 and apdlf=5 means that in the first two partitions we applied the corresponding condition with clf, while apdlf has been employed in the subsequent 5 partitions (clf=0 and apdlf=7 is equivalent to the progressive approach with apdlf, reported in Table 11).

The rate of cleared uncertainty region refers only to the clearable tiles (those not containing an unstable closed-loop model found by gridding). As expected, it is confirmed that the FD-cμ relaxation is the only one that has been able to clear all the clearable tiles, at the price of a higher computational time. When comparing times, it turns out that the adaptation has proved to be effective for both DS-ds and FD-cdμ. On the contrary, it has led to an increase of computational

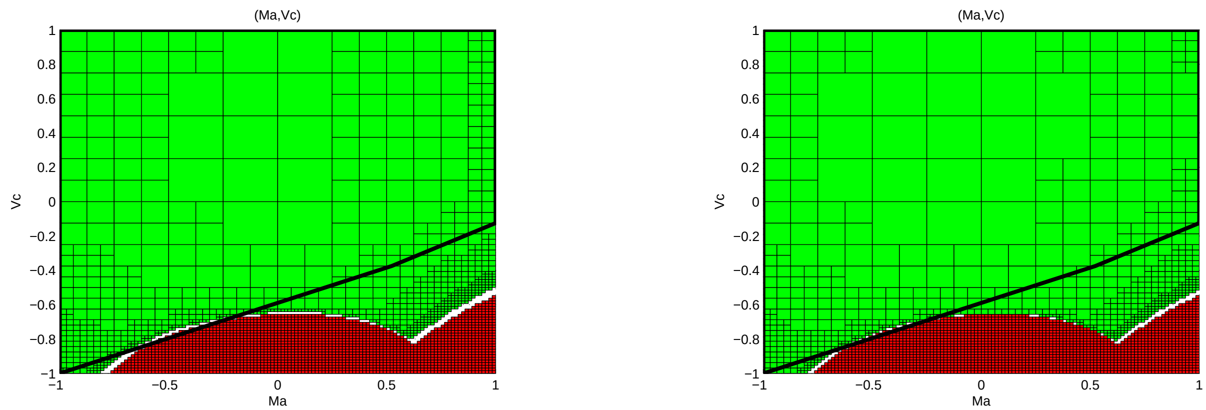

a) b)

Figure 1: a) Clearance by partitioning using DS-ds and clf. b) Clearance by partitioning using Ds-ds and apdlf.

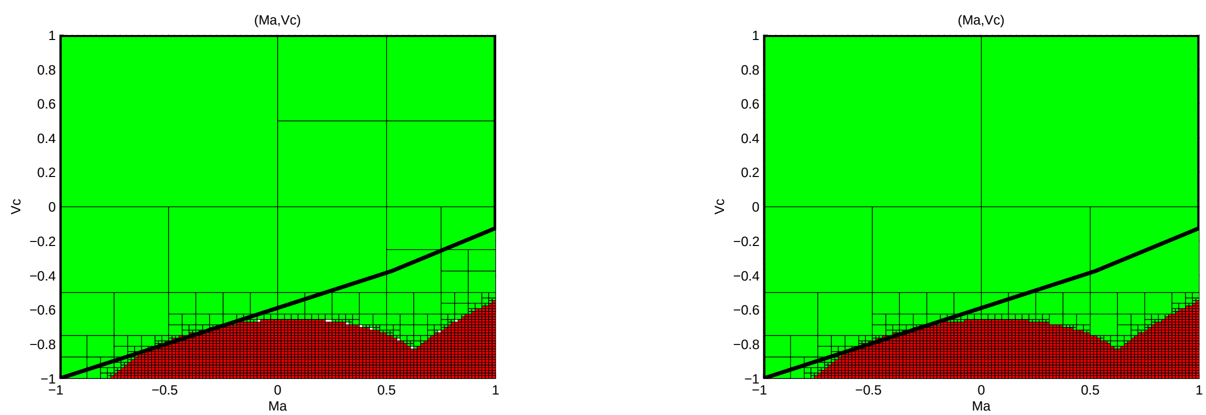

a) b)

Figure 2: a) Clearance by partitioning using FD-cμ and clf. b) Clearance by partitioning using FD-cμ and apdlf.

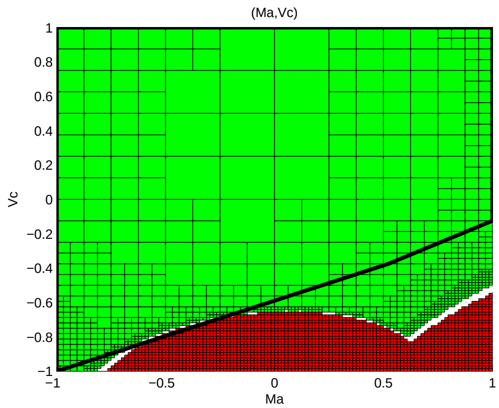

a)

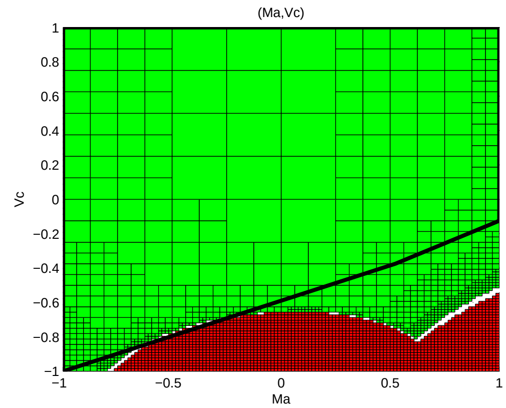

b)

Figure 3: a) Clearance by partitioning using FD-cdμ and clf. b) Clearance by partitioning using FD-cdμ and apdlf.

times for FD-cμ. Adaptation on the WBQ-dM condition has not been performed, because it is known a priori that WB-dN is as conservative as WBQ-dM, being the uncertainty domain symmetric after the reparameterization.

Method	clf	apdlf	Rate	NOPs	Time (h:m:s)	Time/OP (h:m:s)
DS-dS	0	7	0.9931	1030	24 : 35 : 25	0 : 1 : 25
	2	5	0.9931	1042	27 : 27 : 54	0 : 1 : 34
	4	3	0.9931	1110	25 : 20 : 0	0 : 1 : 22
	6	1	0.9931	1236	20 : 10 : 37	0 : 0 : 58
FD-cμ	0	7	1	174	30 : 9 : 45	0 : 10 : 24
	2	5	1	179	31 : 19 : 19	0 : 10 : 29
	4	3	1	188	32 : 21 : 30	0 : 10 : 19
	6	1	1	206	36 : 5 : 11	0 : 10 : 30
FD-cdμ	0	7	0.9921	1202	20 : 59 : 54	0 : 1 : 2
	2	5	0.9921	1214	23 : 13 : 35	0 : 1 : 8
	4	3	0.9921	1266	21 : 18 : 30	0 : 1 : 0
	6	1	0.9921	1362	15 : 39 : 18	0 : 0 : 41

Table 12: Adaptive tiling: `MV` model.

Remark 4.1 *On the whole, the results show that it is not possible to establish a priori which combination of robustness condition, relaxation and structure of the Lyapunov function will give the best performance in terms of overall computational time, because this depends on the trade-off between computational burden and conservatism of each condition, whose impact may in turn depend on the considered example. Experience accumulated in employing the sufficient conditions in the clearance process indicates that the FD-cμ method is the most powerful one among those* *implemented, but it may sometime require an excessive computational effort. On the other hand, the FD-cdμ, DS-dS and WBQ-dM relaxations often provide a good trade-off between computational complexity and conservatism (see e.g., both progressive and adaptive results on the MV model). Concerning the selection of the structure of the Lyapunov function, starting with clf and then switching to apdlf to clear only the "most difficult" tiles, as in the adaptive approach, has proven to be useful in several cases.*

5 Results on un-piloted stability of nonlinear models

In this section we report results obtained by applying the proposed techniques on some LFR models described in Section 3.4, representing the longitudinal nonlinear closed-loop aircraft dynamics.

5.1 `CL_lon_nl_AC_#_b` models

The uncertain flight parameters in this class of models are cg and $mass$. The other flight parameters ($mach$, V_{CAS}) are set to their corresponding nominal values, and the dead-zones are set to zero.

The analysis utilized progressive tiling approach employing FD-cμ method, with affine parameter-dependent Lyapunov functions (apdlf). Tables 13 and 14 summarize the analysis results for a subset of the 16 available LFRs. Table 13 refers to the standard robust stability analysis, while Table 14 concerns "weak stability" analysis, which allows for the presence of slowly divergent modes (corresponding to right shifting the imaginary axis by $\log(2)/6$). The first column (*Model*) represents the model analyzed. The second column (*NOPs*) denotes the number of optimization problems that have been solved (i.e., the number of tiles attempted to be cleared). The third column (t) provides the time elapsed in the course of the clearance procedure, whereas the fourth column (t/OP), shows the average time elapsed per optimization problem. All times are shown in hour:minute:second (h:m:s) format, and are referred to computations performed on an Intel XEON 5150 processor with 4 GB RAM.

The ratio (in %) of the cleared domain to the whole uncertainty domain is given in column *Cleared*. The percentage of the whole uncertain parameter domain, which was found to host closed-loop unstable models after gridding, is given in column *Unstable*. The column *Unknown* shows the percentage of the whole uncertainty domain which could not be defined as unstable after gridding, yet with the tested method it could not be certified as cleared either.

It can be observed that when using the standard notion of stability, unstable models have been found almost everywhere within the flight uncertainty domain. For some models, the clearance process lasted hours as a fine tiling has been required (see e.g., Figures 4a and 5a). Conversely, when "weak stability" is considered (i.e., slowly divergent modes are allowed), all models are fully cleared by solving one single optimization problem, without tiling the uncertainty domain. The computational times are in the order of few minutes. This testifies that slowly divergent modes are indeed present in the closed-loop system and motivated us to address only "weak stability" in the subsequent analysis.

5.2 `CL_lon_nl_AC_#_a` models

This class of models treats $mach$ and V_{CAS} as uncertain flight parameters, the other uncertain parameters (Xcg, $mass$) are set to their corresponding nominal values, and the dead-zones are set to zero.

Model	NOPs	t (h:m:s)	t/OP (h:m:s)	Cleared (%)	Unstable (%)	Unknown (%)
CL_lon_nl_AC_1_b	8	0:49:8	0:6:8	0.195	99.805	0.0
CL_lon_nl_AC_2_b	69	4:26:28	0:3:51	3.442	96.558	0.0
CL_lon_nl_AC_5_b	91	6:35:25	0:4:20	9.839	90.161	0.0
CL_lon_nl_AC_6_b	57	3:40:39	0:3:52	2.20	97.80	0.0
CL_lon_nl_AC_9_b	1	0:4:24	0:4:24	0.024	99.976	0.0
CL_lon_nl_AC_10_b	5461	0:6:55	0:0:0	0.0	100.0	0.0
CL_lon_nl_AC_13_b	14	1:1:16	0:4:22	0.488	99.512	0.0
CL_lon_nl_AC_14_b	5461	0:6:2	0:0:0	0.0	100.0	0.0

Table 13: Clearance analysis for CL_lon_nl_AC_#_b models: standard robust stability analysis.

Model	NOPs	t (h:m:s)	t/OP (h:m:s)	Cleared (%)	Unstable (%)	Unknown (%)
CL_lon_nl_AC_1_b	1	0:4:13	0:4:13	100.0	0.0	0.0
CL_lon_nl_AC_2_b	1	0:4:17	0:4:17	100.0	0.0	0.0
CL_lon_nl_AC_5_b	1	0:3:27	0:3:27	100.0	0.0	0.0
CL_lon_nl_AC_6_b	1	0:3:17	0:3:17	100.0	0.0	0.0
CL_lon_nl_AC_9_b	1	0:3:13	0:3:13	100.0	0.0	0.0
CL_lon_nl_AC_10_b	1	0:7:4	0:7:4	100.0	0.0	0.0
CL_lon_nl_AC_13_b	1	0:3:13	0:3:13	100.0	0.0	0.0
CL_lon_nl_AC_14_b	1	0:4:22	0:4:22	100.0	0.0	0.0

Table 14: Clearance analysis for CL_lon_nl_AC_#_b models: "weak stability".

The "weak stability" analysis utilized progressive tiling approach employing FD-cμ method, with affine parameter-dependent Lyapunov functions (apdlf). Table 15 summarizes the analysis results for the models considered. Figures 6-7 report the results of the analysis and the actual flight envelope boundaries (denoted by thick black lines).

Model	NOPs	t (h:m:s)	t/OP (h:m:s)	Cleared (%)	Unstable (%)	Unknown (%)
CL_lon_nl_AC_2_a	110	114:31:19	1:2:27	96.14	3.86	0.0
CL_lon_nl_AC_5_a	33	47:23:31	1:26:10	97.93	2.07	0.0

Table 15: Clearance analysis for CL_lon_nl_AC_#_a models.

It can be observed that the computational times have significantly increased with respect to CL_lon_nl_AC_#_b models, due to the larger dimension of the LFR Δ block. However, it can be noticed that most of the time is spent in the attempt to clear regions close to the stability boundary, requiring a much finer partitioning, which lie outside the actual flight envelope of interest. This information has been kept in this example, in order to show that the partitioning technique allows one to obtain a detailed approximation of the robust stability domain. In the following analysis,

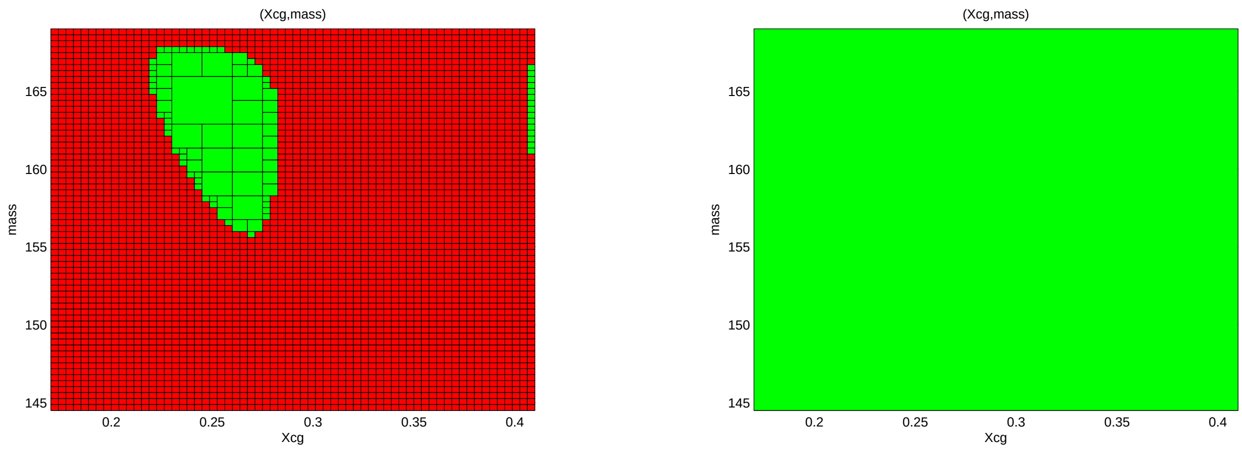

a) b)

Figure 4: a) Standard robust stability analysis of `CL_lon_nl_AC_5_b`. b) Robust "weak stability" analysis of `CL_lon_nl_AC_5_b`.

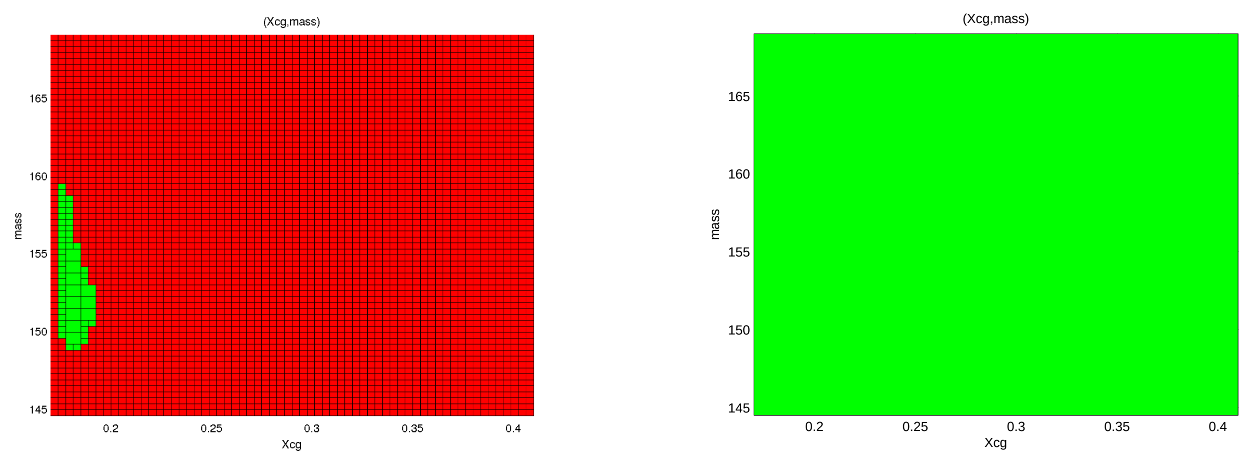

a) b)

Figure 5: a) Standard robust stability analysis of `CL_lon_nl_AC_6_b`. b) Robust "weak stability" analysis of `CL_lon_nl_AC_6_b`.

we will exploit the option *FE restriction*, present in the GUI [16], ensuring that the tiles which are completely outside the flight envelope are omitted from the analysis.

5.3 `CL_lon_nl_AC_#_c` models

In this class of models, all flight parameters are set to their corresponding nominal values, except the four dead-zones PA_DQ_DZ, PC_DQ_DZ, RA_DQ_DZ and RC_DQ_DZ, which are treated as sector-bounded nonlinearities.

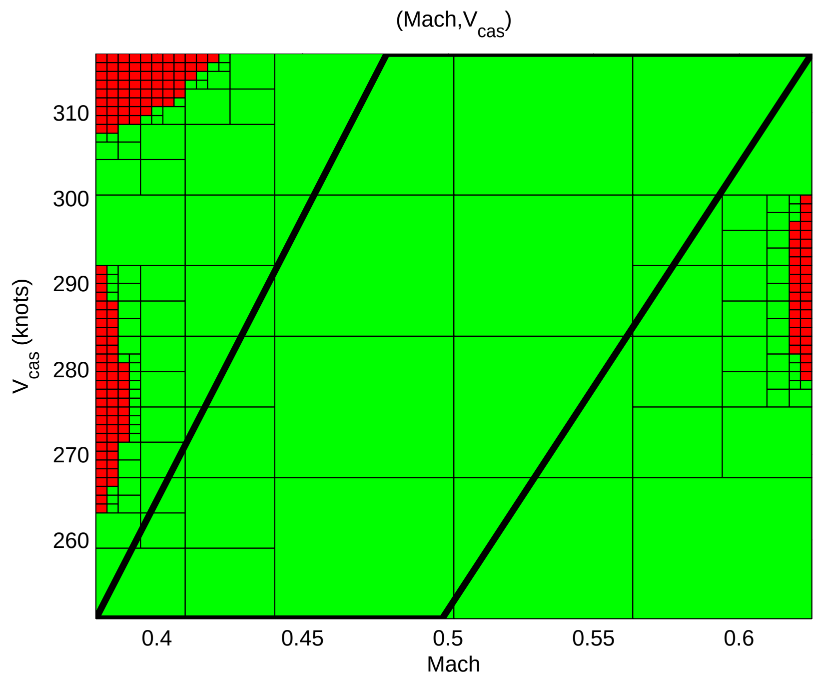

Figure 6: Robust "weak stability" analysis of `CL_lon_nl_AC_2_a`.

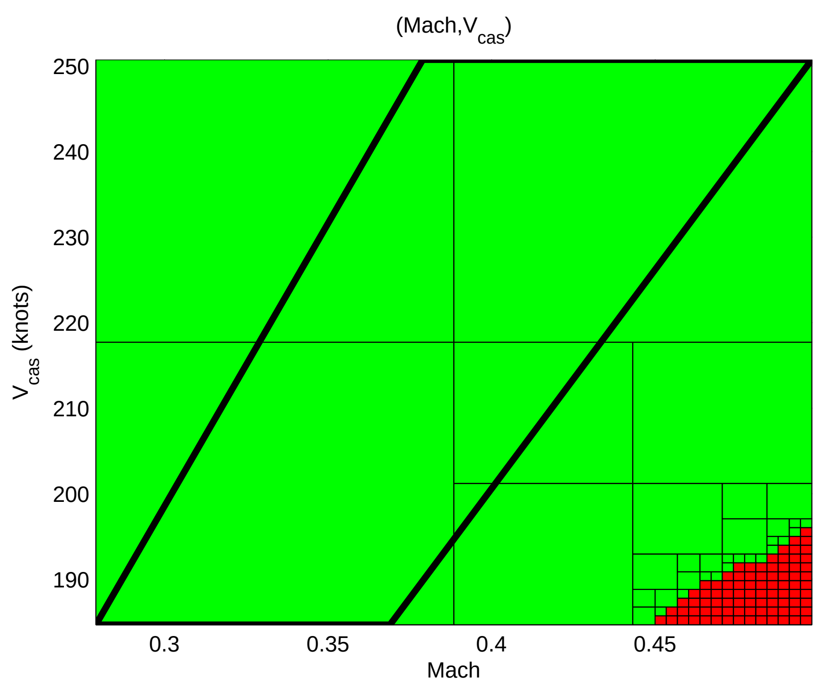

Figure 7: Robust "weak stability" analysis of `CL_lon_nl_AC_5_a`.

After performing analysis of the models with FD-cμ method, common Lyapunov function (clf) and dead-zones considered as sector-bounded uncertainties in the sector $[0, 1]$, none of the considered models have been cleared. Moreover, in all cases it has been possible to find constant values in the interval $[0, 1]$, for the dead-zones parameters, such that the resulting models have eigenvalues with real part greater than $\log(2)/6$. For example, in model `CL_lon_nl_AC_1_c`, if $PA\_DQ\_DZ = PC\_DQ\_DZ = RA\_DQ\_DZ = 0$ and $RC\_DQ\_DZ = 0.8$, one obtains a $\mathbf{A}(\theta)$ matrix in (2) with a pair of conjugate eigenvalues whose real part is $0.1290 > \log(2)/6$.

In order to check for robust stability of models with smaller sector bounds, the dead-zones have been considered as sector-bounded uncertainties, within the sector $[0, \gamma]$. Table 16 reports the maximum values of γ for which robust "weak stability" has been certified by applying the FD-cμ method. These values of γ allow one to compute the maximum ranges of the input signals of the dead-zones for which the system remains stable.

Model	γ
`CL_lon_nl_AC_1_c`	0.62
`CL_lon_nl_AC_2_c`	0.64
`CL_lon_nl_AC_5_c`	0.62
`CL_lon_nl_AC_9_c`	0.60
`CL_lon_nl_AC_13_c`	0.60

Table 16: Maximum values of γ for which `CL_lon_nl_AC_#_c` models have been cleared ("Weak stability").

The same clearance procedure has been applied to LFR models with dead-zones PA_DQ_DZ and PC_DQ_DZ set as uncertain parameters, sector-bounded in sector $[0, 1]$, and all other parameters (including rate limiter dead-zones: RA_DQ_DZ, RC_DQ_DZ) set to their nominal values. All such models have been cleared. On the other hand, LFR models accommodating only RA_DQ_DZ, RC_DQ_DZ dead-zones, and with all the remaining parameters (including the actuator dead-zones PA_DQ_DZ and PC_DQ_DZ) set to their nominal values, have not been cleared. This suggests that the rate limiter dead-zones play a critical role in the clearance analysis.

In [21, 22] several approaches have been proposed to address robust stability of systems with dead-zones. In particular, [22] provides LMI conditions for global exponential stability, which exploit information on the time derivative of the saturated signals and a generalized Lur'e-Postnikov Lyapunov function. Unfortunately, also this technique was not able to clear any model in the `CL_lon_nl_AC_#_c`. Then, motivated by the local stability results in Table 16, we applied the regional analysis techniques proposed in [21], in order to estimate the region of attraction of the origin in the state space. Two approaches have been considered, which are based on the embedding of the LFR with dead-zones either in a polytopic differential inclusion (PDI), or a norm-bounded differential inclusion (NDI). By using these approaches, it has been possible to certify the regional stability of the systems reported in Table 16 and to obtain a non trivial (spherical) estimate of the region of attraction. The radius α of the spherical stability region is reported in Table 17, for the two considered approaches. As expected, the approach based on PDI embedding turned out to be slightly less conservative.

The extension of the techniques presented in [21,22] to LFRs containing both uncertain parameters and dead-zones in the Δ block is a subject of ongoing research.

Model	α (PDI)	α (NDI)
CL_lon_nl_AC_1_c	1.7998	1.7927
CL_lon_nl_AC_2_c	2.9506	2.9372
CL_lon_nl_AC_5_c	1.7867	1.7795
CL_lon_nl_AC_9_c	1.9234	1.9143
CL_lon_nl_AC_13_c	1.92	1.9107

Table 17: Estimation of the stability radius α of CL_lon_nl_AC_#_c models.

5.4 CL_lon_nl_AC_#_d models

This class of models treats as uncertain parameters *cg* and *mass*, and, as sector-bounded uncertainties, the dead-zones related to the elevator position limiters *PA_DQ_DZ* and *PC_DQ_DZ*.

The results obtained by applying the FD-cμ method with clf, for robust "weak stability" with threshold log(2)/6, are given in Table 18. Here the times refer to computations performed on an Intel Core2 Duo processor with 2 GB RAM.

Model	NOPs	t (h:m:s)	t/OP (h:m:s)	Cleared (%)	Unstable (%)	Unknown (%)
CL_lon_nl_AC_1_d	1	0:46:26	0:46:26	100.0	0.0	0.0
CL_lon_nl_AC_5_d	1	0:38:11	0:38:11	100.0	0.0	0.0
CL_lon_nl_AC_9_d	1	0:33:44	0:33:44	100.0	0.0	0.0

Table 18: Clearance analysis for CL_lon_nl_AC_#_d models.

It is worth remarking that these models have been fully cleared by solving one single optimization problem, i.e., no partitioning of the uncertainty domain, including *cg* and *mass*, has been necessary (although up to 6 partitions have been allowed for such parameters).

5.5 CL_lon_nl_AC_#_e models

These LFR models include *mach* and V_{CAS} as uncertain flight parameters, and as sector-bounded uncertainties, the dead-zones related to the elevator position limiters *PA_DQ_DZ* and *PC_DQ_DZ*. Results of "weak stability" analysis, using FD-cμ method with clf, are reported in Table 19.

Model	NOPs	t (h:m:s)	t/OP (h:m:s)	Cleared (%)	Unstable (%)	Unknown (%)
CL_lon_nl_AC_2_e	21	31:45:29	1:30:44	100.0	0.0	0.0
CL_lon_nl_AC_5_e	5	6:4:19	1:12:51	100.0	0.0	0.0

Table 19: Clearance analysis for CL_lon_nl_AC_#_e models.

Both the considered models have been fully cleared, by exploiting partitioning with respect to the time-invariant flight parameters *mach* and V_{CAS}. The resulting tiling patterns are drawn in

Figures 8 and 9. It is interesting to compare the slightly different tiling patterns (within the flight envelope) obtained for models `CL_lon_nl_AC_5_a` (Figure 7) and `CL_lon_nl_AC_5_e` (Figure 9). This is clearly induced by the presence of dead-zones in the latter model, which makes the clearance problem more difficult.

From Table 19, it can be noticed that the computational times are the order of several hours. This is due to the fact that Δ blocks have dimensions around 80. In this case, the use of the FE restriction (which allows to exclude tiles outside the polytopic flight envelope) has proven to be very useful.

6 Final remarks

The research activity within WP2.3 of the `COFCLUO` project has addressed the study and application of Lyapunov-based robustness analysis techniques to two clearance problems concerning the closed-loop longitudinal dynamics of a civil aircraft.

The clearance problems have been cast as robust stability problems and three different sufficient conditions proposed in the literature have been considered. The choice of the conditions has been driven by the fact that the uncertainty models developed within the project were in LFR form. The results obtained indicate that there is a key trade-off between performance and computational burden. This is apparent when robustness conditions are applied within the progressive tiling strategy. Relaxed conditions, which are conservative if applied directly to the entire uncertainty region, may perform much better on smaller subregions. This, however, requires the solution of a large number of LMI optimization problems. The size of the tiles, the number of partitions of the region under analysis, the structure of the multipliers and/or the Lyapunov matrices turn out to be key tuning "knobs" in this respect.

Although it is difficult to devise an a priori strategy for choosing the "best" robustness analysis technique, based on experience accumulated in the testing of the clearance software and in view of the analysis results, a combined use of structurally simple multipliers in either the FD or DS method, with an affine parameter-dependent Lyapunov function seems to offer a reasonable compromise between conservatism and computational feasibility.

The results obtained so far are by no means exhaustive and there are several open issues to be addressed in future research activities. Some of them can be briefly summarized as follows.

- Robustness analysis of LFR models including memoryless nonlinearities is currently the subject of active research in the control field. It is believed that the use of such techniques, combined with those considered in this report, may significantly reduce the conservatism in clearance problems like un-piloted stability or turn coordination for nonlinear models.

- A possible alternative approach to robustness analysis of models in LFR form concerns the use of LPV models, which can be generated by exploiting the model reduction tools developed in [23]. Promising preliminary results have been obtained by applying to these LPV models standard quadratic stability conditions, or linearly parameter-dependent Lyapunov functions (e.g., [24]). Numerical tests are ongoing to verify the computational feasibility of these techniques.

- The robustness techniques presented in this report may provide a valuable tool for validating the LFR modeling process. Indeed, one of the key points to be addressed is the reliability of

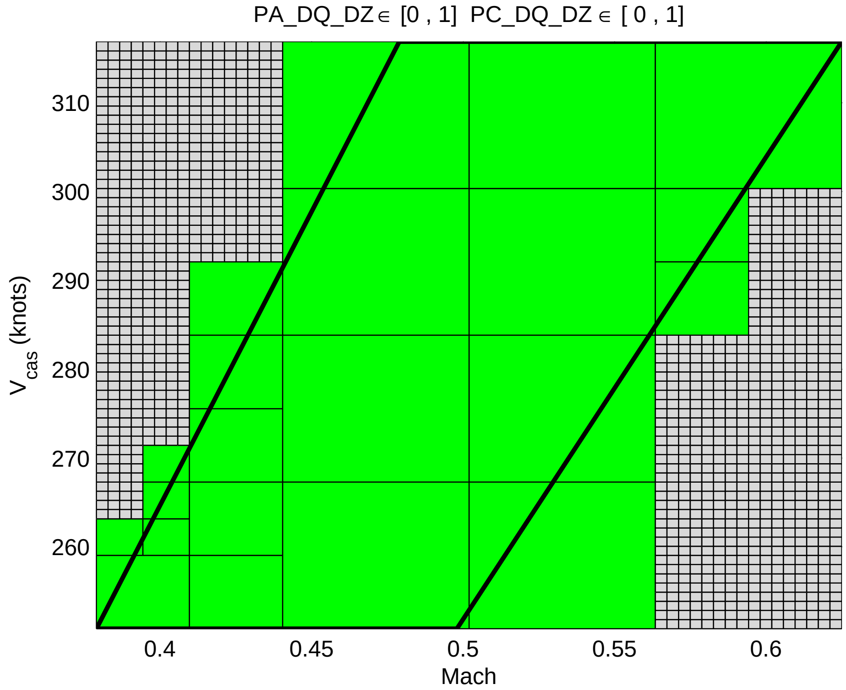

Figure 8: Robust "weak stability" analysis of `CL_lon_nl_AC_2_e`.

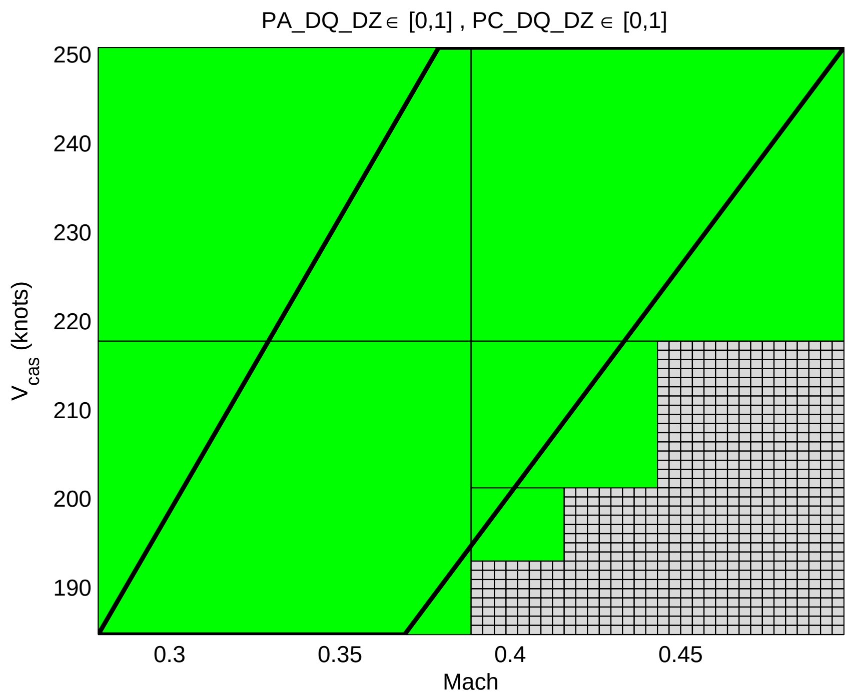

Figure 9: Robust "weak stability" analysis of `CL_lon_nl_AC_5_e`.

these LFRs, i.e. their potential in representing all the aircraft dynamics of interest, within the considered flight envelope and for all admissible values of the uncertain parameters. By comparing the results of Lyapunov-based robust stability analysis with those obtained by applying the baseline solution (usually based on gridding of the fligh/uncertainty domain, see [25]), it will be possible to single out the most significant discrepancies between the physical aircraft models used so far in industrial clearance, and the LFR models developed within the `COFCLUO` project. This will provide guidelines for trading off model accuracy and complexity in the LFR modeling process.

Acknowledgment

The authors of Part I would like to thank Enrica Camparini for her help in preparing this document.

Part II

μ-analysis based robustness analysis for clearance problems

Author: Clément Roos (ONERA)

7 Introduction

Before an aircraft can be tested in flight, it has to be proven to the authorities that the flight control system is reliable, *i.e.* it has to go through a certification and qualification process. An important part of this process is the clearance of flight control laws. It must notably be shown that the control laws provide sufficient stability margins to guarantee a safe operation of the aircraft over the entire flight envelope and for all admissible parametric variations. Clearance problems for both civilian and military aircraft can be formulated as robustness analysis problems, where a set of suitably defined clearance criteria must be checked to lie within certain limits for all possible aircraft configurations and flight conditions. The most common clearance criteria are related to aircraft stability, handling, loads and performance [26].

The current industrial approach consists in gridding the parametric domain, and checking the considered criteria at each point of the grid [25]. The main drawback of this strategy is that clearance is restricted only to the considered grid points and nothing can in principle be assessed for the remaining points in the parametric domain. Moreover, significant time and money is frequently spent on this task. Enhancement would be provided by automated search of worst-case points. Some techniques, such as μ-analysis, could be efficiently applied for this purpose, since they allow to determine whether clearance requirements are fulfilled on a continuous parametric domain. Such an approach has been investigated by ONERA in the context of the COFCLUO project.

The modeling methodology introduced in [13, 14] and the clearance tool presented in [16, 18] are the two main stages towards the development of a modeling and optimization tool dedicated to the clearance of stability criteria, which is able to meet the industrial needs specified in [25]. In this context, the purpose of this document is twofold. The work performed by ONERA during the project is first summarized in section 8. The way how the different contributions can be efficiently combined and implemented to be incorporated in an industrial process is then discussed in section 9.

8 Overview of the work performed by ONERA

The work performed by ONERA during the COFCLUO project is summarized below. It mainly aims at developing an efficient method based on μ-analysis to evaluate some of the clearance criteria that need to be assessed during the certification process of an aircraft. Efforts are notably put on the eigenvalue and the stability margin criteria [9, 27] for high-order flexible models [12].

1. In the aeronautical industry, the robustness properties of an aircraft are usually assessed using intensive and time-consuming simulations. Fortunately, several optimization techniques can be implemented and applied for clearance of flight control laws, in order to improve the efficiency and reliability of the certification process. Some of them, such as μ-analysis, require the considered models to be written as Linear Fractional Representations (LFR), which is unfortunately not the case of the aeroelastic models available in an industrial context. A whole methodology is thus proposed in [13, 14] to convert a set of numerical flexible aircraft models into a suitable LFR which depends on the aircraft configuration and the flight conditions. This is a challenging issue, since the size of the initial models is very large and the state vector does not have the same physical meaning for the whole model set [12]. Nevertheless, several open-loop longitudinal and lateral LFRs are obtained, which are representative of the aircraft behavior in the sense that their eigenvalues and frequency responses almost exactly

match those of the initial flexible models. Moreover, their complexity proves compatible with the use of robustness analysis tools.

2. A strategy is also detailed in [14], which allows to generate some low-order LFRs of both longitudinal and lateral controllers. All the Matlab tools that are necessary to build either linear of nonlinear interconnections and to validate the resulting closed-loop LFRs are available on the COFCLUO portal.

3. Two efficient algorithms based on μ-analysis are then proposed in [16,18,28] to compute either a guaranteed robustness margin for a high-order LTI plant with numerous uncertainties, or a guaranteed stability domain for a high-order (possibly uncertain) LPV plant. Some possible extensions and variations are highlighted, which allow to handle the trade-off between conservatism and computational time. The stress is also put on the way these tools can be more widely exploited to evaluate both the eigenvalue and the stability margin criteria.

4. An easy-to-use Matlab package implementing the aforementioned algorithms and dedicated to the evaluation of the eigenvalue and the stability margin criteria is finally described in [16] and is available on the COFCLUO portal. Numerous tests show that the proposed clearance tool allows to handle high-order flexible plants that cannot be analyzed rigorously using classical methods. Indeed, conservatism is easily mastered and computational time remains quite reasonable, even if very demanding problems are considered.

Another clearance requirement is to show that the flight control laws do not cause excessive damage during a reference flight, in the sense that the fatigue due to mechanical stresses undergone by the aircraft servomechanisms does not exceed a given threshold. In this context, a way to formulate and evaluate the damage criterion has been proposed by ONERA.

- A mathematical formulation of the damage criterion is first introduced in [27] and then implemented in [29]

- The damage criterion is a nonlinear function of the standard deviations of the deflections and the deflection rates of the actuators. It is thus very sensitive to the saturations of the actuators. Nevertheless, standard deviations are easily computed only in a linear context. Some attention must thus be paid to the linearization of these saturations. A stochastic technique is proposed in [30] to carry out this task.

9 Incorporation in an industrial process

The modeling methodology proposed in [13, 14] and the clearance tool presented in [16, 18] are the two main stages towards the development of a modeling and optimization tool dedicated to the clearance of stability criteria, which is able to meet the industrial needs specified in [25]. The way how they can be efficiently combined and implemented to be incorporated in an industrial process is discussed in this section.

9.1 Validation of the LFRs and evaluation of the modeling error

The evaluation of both the eigenvalue and the stability margin criteria consists in examining the position of the eigenvalues of a suitable closed-loop LFR with respect to the imaginary axis. In this context, it seems natural to use a modal indicator to quantify the modeling error, and thus the accuracy, of this LFR before invoking the clearance tool. This is a necessary precaution, since several reductions and other simplifying operations are usually performed to generate an LFR, whose size is compatible with the use of the analysis tools, but which can be quite different from the reference models.

Assume that the modeling methodology introduced in [13, 14] has been applied to get an LFR. The latter depends on the interpolation of a set of N component models defined on a grid, which are supposed to be representative of the real aircraft. Thus, it seems natural to compare the real parts of the eigenvalues of the LFR and of the component models at each point of the grid. The modeling error can then be defined as follows:

$$\epsilon = \max_i \max_j \left| \Re \left(\lambda^{ij} - \lambda^{ij}_{ref} \right) \right| \tag{12}$$

where λ^{ij} and λ^{ij}_{ref} denote the j^{th} eigenvalue of the LFR in the i^{th} grid point and of the i^{th} component model respectively. It is also possible to associate a modeling error to each eigenvalue:

$$\epsilon_j = \max_i \left| \Re \left(\lambda^{ij} - \lambda^{ij}_{ref} \right) \right| \tag{13}$$

Remark 9.1 *Interpolation is usually performed so that the modeling error remains low on the grid, which can lead to an optimistic value of ϵ. A more realistic approach consists first in generating a low-order LFR using a coarse grid and then in computing the modeling error on a denser grid with $\tilde{N} \gg N$ points. Unfortunately, this strategy cannot be applied in the context of the COFCLUO project, since only a very coarse grid is available [9].*

9.2 Integration of the modeling error into the bounds of the criteria

The most convenient way to take into account the modeling error during the analysis process is to incorporate it directly into the bounds of the criteria. More precisely, the idea is to investigate stability with respect to the boundary a truncated sector instead of the imaginary axis:

- If a single modeling error ϵ is computed, the sector reduces to a vertical line, as shown in figure 10.
- Otherwise, an exclusion region is defined for each eigenvalue, as depicted in figure 11, where:

$$m_j = \min_i |\Im(\lambda_{ij})| \quad \text{and} \quad M_j = \max_i |\Im(\lambda_{ij})| \tag{14}$$

  The sector is then defined so as to leave all exclusion regions to its right.

Note that stability can be easily investigated with respect to the boundary of a truncated sector using the clearance tool described in [16].

9.3 Description of the proposed clearance process

In the light of the previous comments, the modeling methodology proposed in [13, 14] and the analysis tools introduced in [16, 18] can now be integrated into a whole clearance process, which is likely to be implemented in an industrial context. It is assumed that a set of N open-loop reference models [12], as well as a reference controller and actuators/sensors models [11] are available.

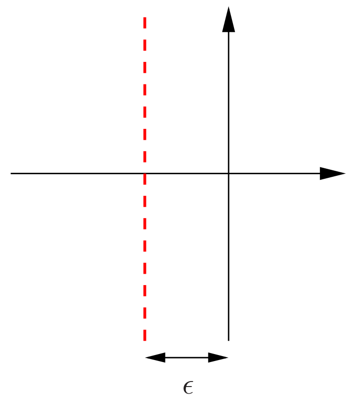

Figure 10: Analysis with respect to a vertical line

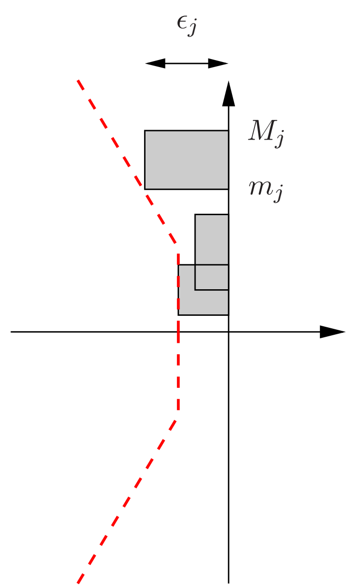

Figure 11: Analysis with respect to the boundary of a truncated sector

Procedure 9.1

1. *Apply the modeling technique described in chapter 4 of [14] to convert the reference controller, as well as the actuators and the sensors models, into LFRs.*

2. *Apply the modeling technique described in chapter 3 of [14] to create a low-order open-loop LFR from the reference set of N component models corresponding to different flight conditions and mass configurations.*

3. *Create a closed-loop LFR and compute the modeling error on a fine grid composed of $\tilde{N} \gg N$ points, as explained in section 9.1.*

4. Incorporate the modeling error into the bounds of the clearance criteria of interest, as described in section 9.2. Evaluate the criteria using the analysis tools introduced in [16, 18]. If the modeling error is too high and results are conservative, increase N and go back to step 2. If some critical regions of the parametric domain cannot be cleared, go to step 5 to modify the reference controller. Otherwise, stop.

5. Modify an elementary gain $K(p)$ of the controller, where p denotes the parameters vector. Let the new gain be written as $\tilde{K}(p) = K(p) + \Delta K(p)$. Perform a simple interpolation, so as to convert $\Delta K(p)$ into an LFR. Incorporate this elementary LFR into the one of the controller and go back to step 3.

Remark 9.2 *Increasing N at step 4 of the aforementioned procedure allows to reduce the modeling error, but is likely to increase the size of the LFR due to higher interpolation orders.*

Remark 9.3 *If the additional term $\Delta K(p)$ remains low compared to $K(p)$, it can be assumed that the modeling error is not modified by the change in the reference controller. A new validation of the closed-loop LFR can thus be avoided, or at least alleviated.*

9.4 Determination of the most critical parametric combinations

The clearance tool described in [16] can be used to evaluate not only the stability but also the performance properties of a closed-loop system. The idea is to investigate stability with respect to a truncated sector instead of the imaginary axis. Such an extension may not be necessary for certification but it can help the control engineers to identify easily the most critical configurations for which performance degradations or even loss of stability are most likely to occur if additional uncertainties or unmodeled dynamics are considered. It also allows to take into account the modeling error resulting from the use of simplified LFRs instead of full-order reference models to perform analysis, as explained in section 9.2. Some results are shown in figure 12 for a closed-loop LFR with two parameters (Mach number M and calibrated airspeed V_{cas}) and for a set of sectors characterized by a relative stability degree $\alpha = -0.168k$ and a damping factor $\xi = 0.0168k$, where k can take several values between 0 and 1 (see [16] for more details). Each of the subdomains, on which stability can be guaranteed, is represented by a yellow rectangle. The stability domain obtained using a standard grid-based approach is also plotted for the sake of comparison (stable and unstable configurations are represented by green dots and red x-marks respectively).
For example, it can be observed that the configuration $(M = -1, V_{cas} = -1)$ cannot be cleared for $k \geq 0.6$. It is thus more critical than $(M = 1, V_{cas} = 1)$, which is in turn more critical than $(M = -1, V_{cas} = 1)$. The size of the stability subdomains also provides a confidence level: the larger a stability subdomain, the higher the guarantee that the real system is actually stable.

9.5 Towards a generalized use of LFRs

At first, the proposed analysis tools can be seen as indicators, which allow to determine quickly the most critical parametric configurations in terms of system stability or performance. In the light of the obtained results, it is then possible to concentrate Monte Carlo simulations on reduced parametric domains, thus decreasing the computational cost. In this perspective, the number of points $\tilde{N}$ used to validate the closed-loop LFR in step 3 of procedure 9.1 must satisfy $\tilde{N} > N$, but not necessarily $\tilde{N} \gg N$.

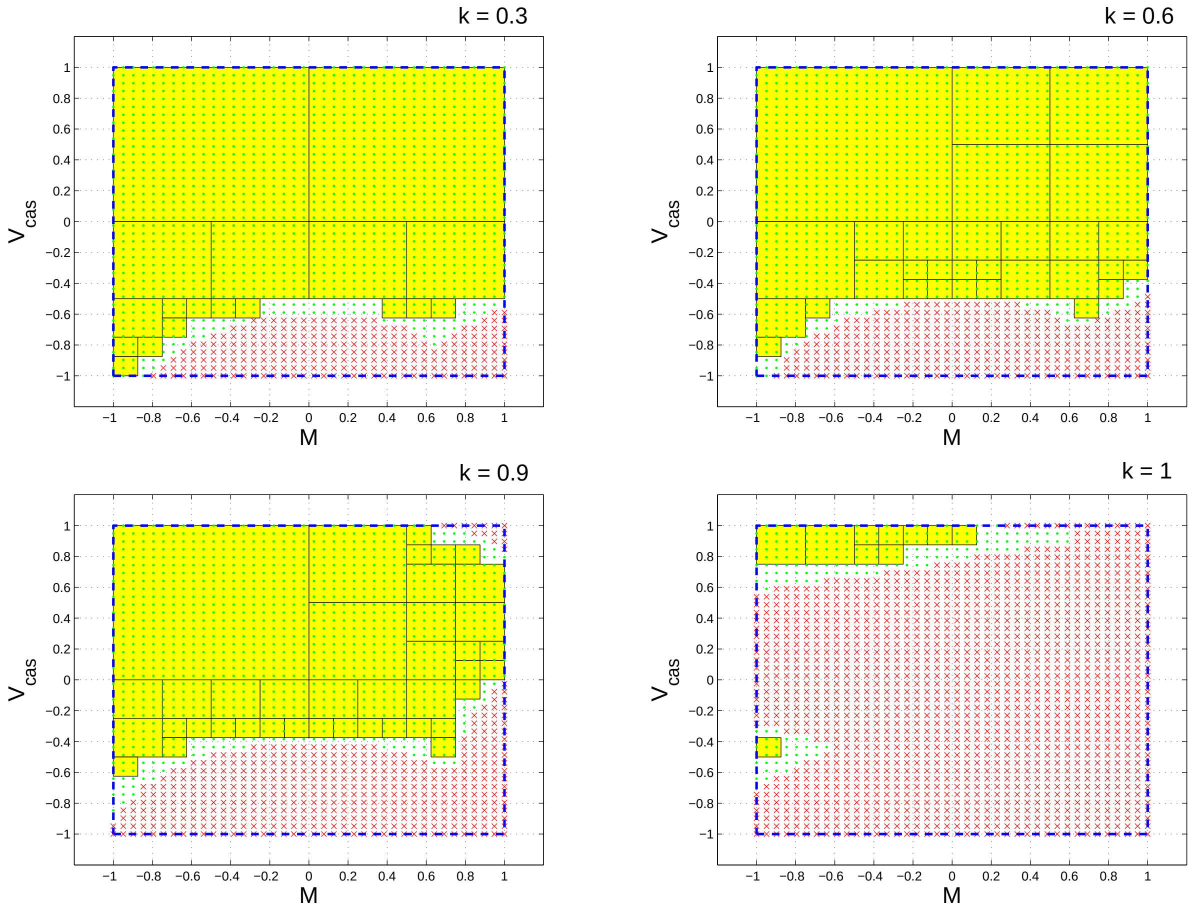

Figure 12: Guaranteed stability domain with respect to the boundary of a truncated sector

Subsequently, it can be considered to use the proposed analysis tools as real validation means, thus allowing to get rid of Monte Carlo simulations to compute guaranteed stability domains. Nevertheless, a thorough validation of the closed-loop LFR becomes necessary to quantify the modeling error as rigorously as possible. Such a validation can be achieved using Monte Carlo simulations, which requires to generate a set of $\tilde{N} \gg N$ models and is thus more computationally involving than before. However, it is worth being emphasized that these simulations only need to be achieved once for the reference controller, but not each time an elementary gain is modified (see remark 9.3). Moreover, several criteria can be evaluated without resorting to any additional Monte Carlo simulations (eigenvalue and stability margin criteria as detained in [16], but also comfort and turbulence loads criteria, provided that the proposed clearance tool is slightly adapted to allow the resolution of skew-μ problems).

The numerous results presented in [16] have demonstrated the benefits of achieving part of the flight control laws clearance using analysis tools based on μ-analysis. Nevertheless, a delicate issue remains in the methodology proposed by ONERA, which deals with the conversion of the open-loop reference models into a suitable LFR. An efficient but quite complicated technique has been introduced in [14], so as to deal with models, whose state vector strongly varies from one parametric configuration to another. But this modeling task usually requires manual intercession. A major improvement would be to adapt the method for creating the reference models, so as to make them more coherent. Indeed, it would be very beneficial if their state vector could be the same for all component models, or at least be perfectly known for all considered parametric configurations, which is far from being the case at the moment. Such an improvement would pave the way for a fully automated modeling and clearance tool.

10 Conclusion and future prospects

The current industrial approach to clearance of flight control laws consists in gridding the parametric domain and checking a set of criteria at each point of the grid. The main drawback of this strategy is that clearance is restricted only to the considered grid points and nothing can be assessed for the remaining points in the parametric domain. Moreover, significant time and money is frequently spent on this task, due to the intensive resort to Monte Carlo simulations.

An efficient strategy has been proposed by ONERA in the context of the COFCLUO project to overcome these limitations. More precisely, the LFR modeling methodology proposed in [13, 14] is combined with the μ-analysis technique introduced in [16, 18] to develop a whole modeling and optimization tool dedicated to the clearance of stability and performance criteria, which is able to meet the industrial needs specified in [25].

It would now be instructive to compare this new approach with a more classical method based on Monte Carlo simulations, which could not be achieved during the project, since no tools were available to build an open-loop reference model in any point of the parametric domain. Finally, it is worth being emphasized that integrating clearance tools based on μ-analysis in an industrial context seems very promising, as demonstrated in [16]. Nevertheless, it cannot reasonably be achieved without reconsidering the whole modeling strategy, so as to integrate LFRs from the very beginning of the process. Such an improvement falls within the competence of Airbus engineers.

References

[1] S. Boyd, L. El Ghaoui, E. Feron, and V. Balakrishnan, *Linear Matrix Inequalities in System and Control Theory.* Studies in Applied Mathematics, SIAM, 1994.

[2] G. Chesi, A. Garulli, A. Tesi, and A. Vicino, "Polynomially parameter-dependent Lyapunov functions for robust stability of polytopic systems: an LMI approach," *IEEE Trans. on Automatic Control*, vol. 50, no. 3, pp. 365–370, 2005.

[3] K. Zhou, J. C. Doyle, and K. Glover, *Robust and Optimal Control.* Prentice Hall Inc., 1996.

[4] F. Wang and V. Balakrishnan, "Improved stability analysis and gain-scheduled controller synthesis for parameter-dependent systems," *IEEE Trans. on Automatic Control*, vol. 47, no. 5, pp. 720–734, 2002.

[5] S. Dasgupta, G. Chockalingam, B. D. O. Anderson, and M. Fu, "Lyapunov functions for uncertain systems with applications to the stability of time varying systems," *IEEE Transactions on Circuits and Systems - I*, vol. 41, no. 2, pp. 93–106, 1994.

[6] M. Fu and S. Dasgupta, "Parametric lyapunov function for uncertain systems: The multiplier approach," in *Advances in Linear Matrix Inequality Methods in Control*, (L. El Ghaoui and S.-I. Niculescu, Eds. Philadelphia, PA: SIAM), 2000.

[7] M. Dettori and C. Scherer, "New robust stability and performance conditions based on parameter dependent multipliers," in *Proc. of 39th IEEE Conf. on Decision and Control*, (Sydney, Australia), pp. 4187–4192, 2000.

[8] Y. Ebihara and T. Hagiwara, "A dilated lmi approach to robust performance analysis of linear time-invariant uncertain systems," *Automatica*, vol. 41, no. 11, pp. 1933–1941, 2005.

[9] Y. Losser, "COFCLUO deliverable D1.1.1 - part 2. Report describing the selected clearance problem," tech. rep., AIRBUS France SAS, 2007.

[10] G. Puyou, "COFCLUO deliverable D1.1.1 - part 1. Report describing the selected clearance problem," tech. rep., AIRBUS France SAS, 2007.

[11] G. Puyou, "COFCLUO deliverable D1.1.2 - Models delivery- part 1- Nonlinear model," tech. rep., AIRBUS France SAS, 2007.

[12] Y. Losser, "COFCLUO deliverable D1.1.2 - Models delivery- part 2- Integral model," tech. rep., AIRBUS France SAS, 2007.

[13] C. Roos, "Generation of flexible aircraft LFT models for robustness analysis," in *Proc. of the 6-th IFAC Symposium on Robust Control Design*, (Haifa, Israel), 2009.

[14] C. Roos, C. Döll, S. Hecker, and A. Varga, "COFCLUO deliverable D1.4.7: Preliminary LFT models for nonlinear behaviour and complete model of aircraft linear dynamics," tech. rep., ONERA - France, DLR - Germany, December 2008.

[15] S. Hecker, "Corrected LFT models for the longitudinal COFCLUO nonlinear A/C model - (in addition to D1.4.7)," tech. rep., DLR - Germany, May 2009.

[16] A. Masi, E. Turkoglu, D. Benedettelli, S. Paoletti, A. Garulli, C. Roos, and J.-M. Biannic, “COFCLUO deliverable D2.3.4 - Final sofware developed,” tech. rep., University of Siena - Italy, ONERA - France, January 2010.

[17] V. M. Popov, “Absolute stability of nonlinear systems of automatic control,” *Automation and Remote Control*, vol. 22, pp. 857–875, 1962.

[18] A. Garulli, A. Masi, S. Paoletti, E. Turkoglu, J.-M. Biannic, and C. Roos, “COFCLUO deliverable D2.3.3 - New optimisation techniques developed,” tech. rep., University of Siena - Italy, 2009.

[19] J.-F. Magni, “Linear Fractional Representation Toolbox (version 2.0) for use with Matlab,” tech. rep., 2006. http://www.cert.fr/dcsd/idco/perso/Magni/.

[20] J.-M. Biannic and C. Döll, “Simulink handling of LFR-objects,” tech. rep., ONERA, France, 2006. http://www.cert.fr/dcsd/idco/perso/Biannic/.

[21] T. Hu, A. Teel, and L. Zaccarian, “Stability and performance for saturated systems via quadratic and nonquadratic Lyapunov functions,” *IEEE Transactions on Automatic Control*, vol. 51, no. 11, pp. 1770–1786, 2006.

[22] D. Dai, T. Hu, A. Teel, and L. Zaccarian, “Piecewise-quadratic Lyapunov functions for systems with deadzones or saturations,” *Systems & Control Letters*, vol. 58, no. 5, pp. 365–371, 2009.

[23] D. Petersson and J. Löfberg, “COFCLUO deliverable D1.4.6 - Identification of LPV state-space models using H2-minimisation,” tech. rep., Linköping University - Sweden, January 2010.

[24] P. Gahinet, P. Apkarian, and M. Chilali, “Affine parameter-dependent Lyapunov functions and real parametric uncertainty,” *IEEE Trans. on Automatic Control*, vol. 41, no. 3, pp. 436–442, 1996.

[25] G. Puyou, “COFCLUO deliverable D3.1.2 - Baseline solution,” tech. rep., AIRBUS France SAS, 2008.

[26] C. Fielding, A. Varga, S. Bennani, and M. S. (Eds), *Advanced techniques for clearance of flight control laws*. Lecture Notes in Control and Information Sciences, vol. 283, Springer-Verlag, 2002.

[27] A. Varga, A. Garulli, H.-D. Joos, Y. Losser, P. Mouyon, C. Papageorgiou, G. Puyou, and J. Robinson, “Clearance criteria for civil aircraft,” Tech. Rep. COFCLUO D1.2.1, DLR, Germany, July 2007. Available at http://er-projects.gf.liu.se/∼45b09cc68460d.

[28] A. Garulli, A. Masi, S. Paoletti, E. Türkoğlu, and C. Roos, “Report on the review and analysis of the models and clearance criteria,” Tech. Rep. COFCLUO D2.3.2, University of Siena, Italy, April 2008. Available at http://er-projects.gf.liu.se/∼45b09cc68460d.

[29] A. Varga, H.-D. Joos, and P. Mouyon, “Clearance criteria library,” Tech. Rep. COFCLUO D1.2.2, DLR, Germany, January 2008.

[30] H.-D. Joos, S. Hecker, A. Varga, and P. Mouyon, “Trimming and linearization tools for criteria evaluation,” Tech. Rep. COFCLUO D1.3.3, DLR, January 2008.